

Expedited Articles

Novel Tricyclic Poly(ADP-ribose) Polymerase-1 Inhibitors with Potent Anticancer Chemopotentiating Activity: Design, Synthesis, and X-ray Cocrystal Structure

Stacie S. Canan Koch,^{*,†} Lars H. Thoresen,^{‡,§} Jayashree G. Tikhe,[†] Karen A. Maegley,[†] Robert J. Almassy,^{†,||} Jianke Li,^{†,⊥} Xiao-Hong Yu,[†] Scott E. Zook,^{†,¶} Robert A. Kumpf,[†] Cathy Zhang,[†] Theodore J. Boritzki,[†] Rena N. Mansour,^{†,▽} Kanyin E. Zhang,^{†,▽} Anne Ekker,[†] Chris R. Calabrese,[‡] Nicola J. Curtin,[‡] Suzanne Kyle,[‡] Huw D. Thomas,[‡] Lan-Zhen Wang,[‡] A. Hilary Calvert,[‡] Bernard T. Golding,[‡] Roger J. Griffin,[‡] David R. Newell,[‡] Stephen E. Webber,^{†,◆} and Zdenek Hostomsky[†]

Pfizer Global Research and Development, La Jolla/Agouron Pharmaceuticals, Inc., 10770 Science Center Drive, San Diego, California 92121, and University of Newcastle, Newcastle upon Tyne, NE2 4HH, U.K.

Received June 19, 2002

A series of novel compounds have been designed that are potent inhibitors of poly(ADP-ribose) polymerase-1 (PARP-1), and the activity and physical properties have been characterized. The new structural classes, 3,4,5,6-tetrahydro-1*H*-azepino[5,4,3-*cd*]indol-6-ones and 3,4-dihydro-pyrrolo[4,3,2-*de*]isoquinolin-5-(1*H*)-ones, have conformationally locked benzamide cores that specifically interact with the PARP-1 protein. The compounds have been evaluated with in vitro cellular assays that measure the ability of the PARP-1 inhibitors to enhance the effect of cytotoxic agents against cancer cell lines.

Introduction

Poly(ADP-ribose) polymerase-1 (PARP-1: EC 2.4.2.30) is the most abundant and best characterized member of a family of PARP enzymes with important cellular functions.^{1–6} PARP-1, a nuclear enzyme implicated in the maintenance of genomic integrity, consists of three functional domains: an N-terminal DNA-binding domain, a C-terminal catalytic domain, and a central automodification domain. PARP-1 binds to and is activated by DNA strand breaks and catalyzes the synthesis of homopolymers of ADP-ribose from NAD⁺ onto nuclear acceptor proteins. PARP-1 itself is the main protein acceptor (automodification), but the enzyme has also been shown to modify histones, topoisomerases, DNA polymerases, and ligases.^{7,8} The formation of these negatively charged polymers in the vicinity of the DNA nick is thought to cause the electrostatic repulsion of PARP-1 (and histones) from the DNA and to facilitate the recruitment of the base excision repair (BER) complex.⁹ The ADP-ribose polymers formed by PARP are cleaved by the cellular hydrolase poly(ADP-ribose) glycohydrolase (PARG). PARP-1 activation and the

rapid synthesis and degradation of ADP polymers can result in abrupt and profound cellular NAD⁺ depletion.

Cytotoxic drugs or radiation can induce activation of PARP-1, and it has been demonstrated that inhibitors of PARP-1 can potentiate the DNA damaging and cytotoxic effects of chemotherapy and irradiation.¹⁰ Because of the essential function of PARP-1 for cellular repair and survival, we sought to evaluate the potential of novel, potent PARP-1 inhibitors for the treatment of cancer in combination with selected cytotoxic agents.

Inhibitors have been designed to mimic the substrate–protein interactions of NAD⁺ with PARP-1. The inhibitors are theorized to bind to PARP-1 and to prevent polymer formation and hence the electrostatic repulsion of PARP from DNA, thus inhibiting the repair of the DNA strand breaks. This leads to eventual cell death. Early PARP inhibitors were analogues of 3-amino-benzamide (Figure 1).¹¹ It was realized that the benzamide functionality was critical for specific binding to PARP-1, and analogue synthesis indicated that the *s*-trans conformation of the benzamide was the most favorable binding conformation for PARP inhibition.¹² Recent cocrystal structures have confirmed this critical binding mode.¹³ PARP-1 inhibitors have since been designed to lock the benzamide group in this specific *s*-trans conformation.¹⁴ Some examples of PARP-1 inhibitors that incorporate the locked conformation at the amide functionality, with either bicyclic systems (NU1025 and PD128763) or intramolecular hydrogen bonding arrangements (NU1085), are shown in Figure 1. Although some of these PARP-1 inhibitors displayed potent in vitro activity, they lacked specificity, had poor physical properties, had unfavorable pharmacokinetic

* To whom correspondence should be addressed. Phone: (858) 622-7504. Fax: (858) 526-4151. E-mail: stacie.canan@pfizer.com.

[†] Pfizer Global Research and Development, La Jolla/Agouron Pharmaceuticals, Inc.

[‡] University of Newcastle.

[§] Current address: Department of Chemistry, Texas A&M University, College Station, TX.

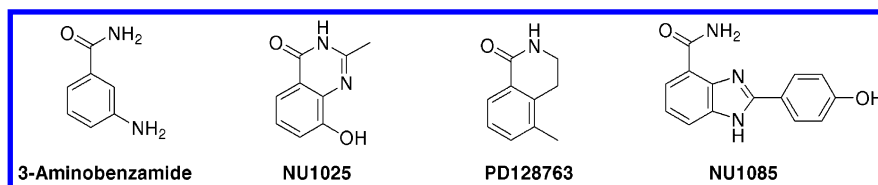
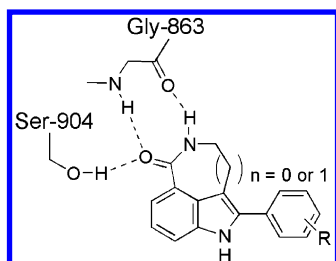
^{||} Current address: Quorex Pharmaceuticals, San Diego, CA 92121.

[⊥] Current address: 8937 Gainsborough Avenue, San Diego, CA 92129.

[¶] Current address: Neurocrine Pharmaceuticals, San Diego, CA 92121.

[▽] Current address: Novartis Genomics Institute, La Jolla, CA 92121.

[◆] Current address: Anadys Pharmaceuticals, San Diego, CA 92121.

**Figure 1.** Examples of reported PARP-1 inhibitors.**Figure 2.** Model of newly designed tricyclic PARP-1 inhibitors.

profiles, or had in vivo side effects that prevented them from being developed further as clinical agents.

Design

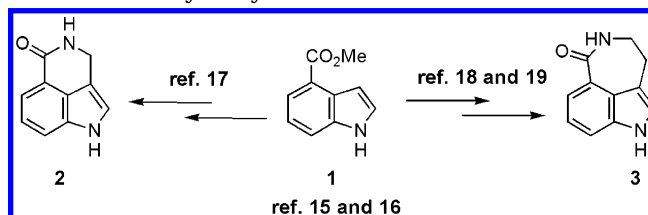
It was our objective to design more potent PARP-1 inhibitors with favorable physical properties and in vivo profiles suitable for preclinical development. We proposed novel tricyclic indole analogues that would structurally restrict the benzamide rotation and allow the optimum interactions with the protein active site (Figure 2). The new PARP-1 inhibitors were designed with a benzamide functionality that is locked in the *s-trans* conformation via a ring connection (i.e., lactam) to an indole core. Modeling studies indicated that these tricyclic systems would allow maximum interaction (three critical hydrogen bonds) of the lactam carbonyl/N-H with the glycine-863 and serine-904 residues at the protein active site. Two tricyclic structures are reported here: the 3,4,5,6-tetrahydro-1*H*-azepino[5,4,3-*cd*]indol-6-ones ([5,6,6]-tricyclic indole lactams) and the 3,4-dihydropyrrolo[4,3,2-*de*]isoquinolin-5-(1*H*)-ones ([5,6,7]-tricyclic indole lactams). The tricyclic design allows for maximum incorporation of diversity by functionalization at the C-2 position of the indole ring. Both the six- and seven-membered lactams were investigated, and we predicted from the modeling studies that the [5,6,7]-system would exhibit the most favorable physical properties (solubility, melting point) and still participate in productive protein interactions with PARP-1 (*vide infra*).

Chemistry

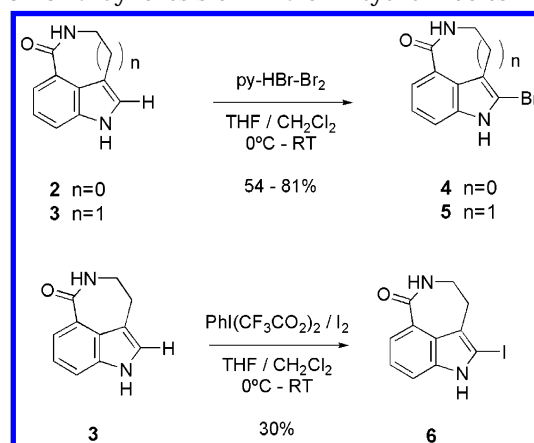
The synthesis of the tricyclic indole lactams utilizes the Leimgruber-Batcho indole cyclization to generate the key 4-carboxyindole intermediate (**1**, Scheme 1) and essentially follows procedures that have been published.^{15,16} The [5,6,6]-tricyclic core, **2**, was prepared as described in the literature by Demerson et al.¹⁷ (Scheme 1). The [5,6,7]-tricyclic core, **3**, was prepared from the 4-carboxyindole by procedures described by Flaugh, Clark, Bowman, and Somei.^{18,19}

The tricyclic intermediates (**2** and **3**) were brominated at the 2-position with pyridinium tribromide to yield the tricyclic bromides **4** and **5** (Scheme 2). The [5,6,7]-

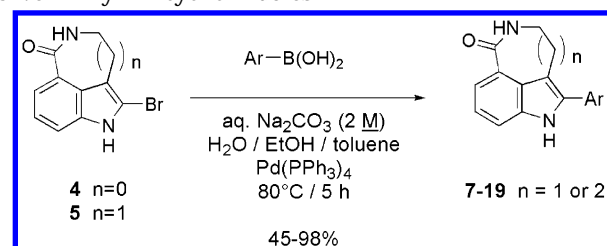
Scheme 1. Key Tricyclic Intermediates



Scheme 2. Synthesis of 2-Halo Tricyclic Indoles



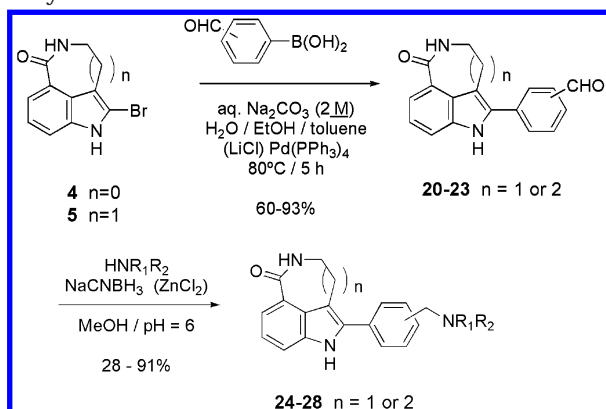
Scheme 3. Palladium-Catalyzed Coupling Reactions To Give 2-Aryl Tricyclic Indoles^a



^a Ar defined in Tables 2 and 6.

tricyclic indole intermediate, **3**, was also iodinated at the 2-position with bis[(trifluoroacetoxy)iodo]benzene and iodine to give the 2-iodo-[5,6,6]-tricyclic indole, **6** (Scheme 2). Each tricyclic bromide underwent Suzuki-type couplings (Scheme 3) with a variety of arylboronic acids to give the 2-aryl-[5,6,7]- or [5,6,6]-tricyclic indole lactams (**7–19**), which were evaluated for PARP-1 activity. Formyl substituted 2-aryl tricyclic indole lactams (**20–23**) were further functionalized through reductive amination with sodium cyanoborohydride and a variety of primary and secondary amines (**24–28**, Scheme 4).

To investigate the critical nature of the lactam functionality in the tricyclic inhibitors, several analogues were prepared to disrupt the hydrogen bonding ability of this group. Scheme 5 illustrates the synthesis of four analogues: methylation (NaH, MeI) of the indole nitrogen to give **29** and the lactam nitrogen to yield the dimethyl analogue **30**; conversion to the thiolactam **31**

Scheme 4. Reductive Amination Procedure To Yield Benzylamines^a^a R₁ and R₂ defined in Tables 3 and 6.

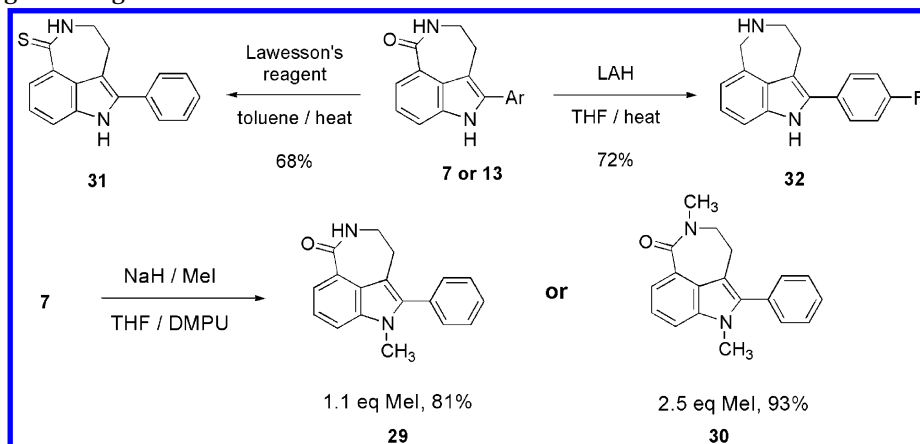
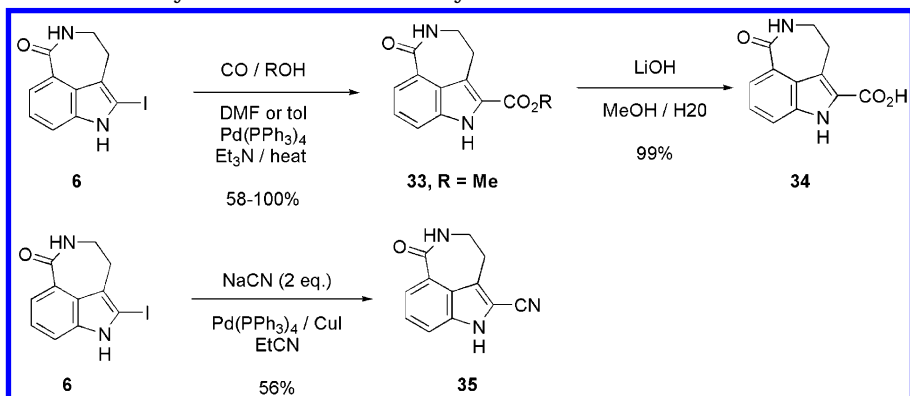
with Lawesson's reagent; and reduction of the lactam carbonyl with LAH to give the azatricycle **32**.

The 2-iodotricycle (**6**) was converted into the 2-carboxy or 2-carbonitrile derivatives by palladium-mediated reactions (Scheme 6). Finally, 2-carbamide analogues were generated from the 2-carboxy intermediate (**33**) by treatment with methylamine in methanol or coupling (HATU) of the acid (**34**) with other primary amines.

Cocrystal Structures

Cocrystal structures of the new tricyclic PARP-1 inhibitors indicate that the lactam functionality can adopt an ideal conformation for multiple interactions with the PARP-1 protein. These specific interactions are

apparent in X-ray cocrystal structures of representative analogues from the [5,6,7]-tricyclic series (compounds **7** and **25**) with the PARP-1 protein (chicken PARP-1 catalytic domain, cPARP-1 CD; see Figures 3 and 4). The critical hydrogen bonds between the lactam functionality and the Gly-863 and Ser-904 residues in this tricyclic series of compounds are apparent in both cocrystal structures, and ideal hydrogen bond distances have been established between the ligand and the protein (2.7–3.0 Å). The nonplanar conformation of the seven-membered lactam most likely contributes to this ideal interaction between the tricyclic ligands and the protein, allowing the lactam carbonyl and –NH to adopt a position closer to the protein residues involved in the hydrogen bonding. Additionally, the cocrystal structure indicates that nearby tyrosine residues (Tyr-907, Tyr-889, and Tyr-896) in the protein likely participate in π – π -type interactions (pseudo-edge-to-face and pseudo-face-to-face) with the indole core and the C-2 aryl substituent. Both structures reveal an ordered water molecule that participates in hydrogen bonding (2.8–3.1 Å) between the indole NH and the important catalytic Glu-988 residue.²⁰ Gln-763 appears to be mobile, and the movement of this residue nicely accommodates the *p*-benzylamine substituent in compound **25**. The cocrystal X-ray structure of the amine compound, **25** (Figure 4), displays other unique changes in the protein conformation. The hydrogen bond between residues Tyr-889 and Asp-766 (see Figure 3) seen in the structure of the C-2 unsubstituted phenyl analogue, **7**, with the PARP-1 protein appears to be broken in the **25** cocrystal structure where the *p*-dimethylamino-

Scheme 5. Analogues Designed To Evaluate Lactam Interactions with PARP-1 Protein**Scheme 6.** Synthesis of 2-Carboxy and 2-Carbonitrile Tricyclic Indoles

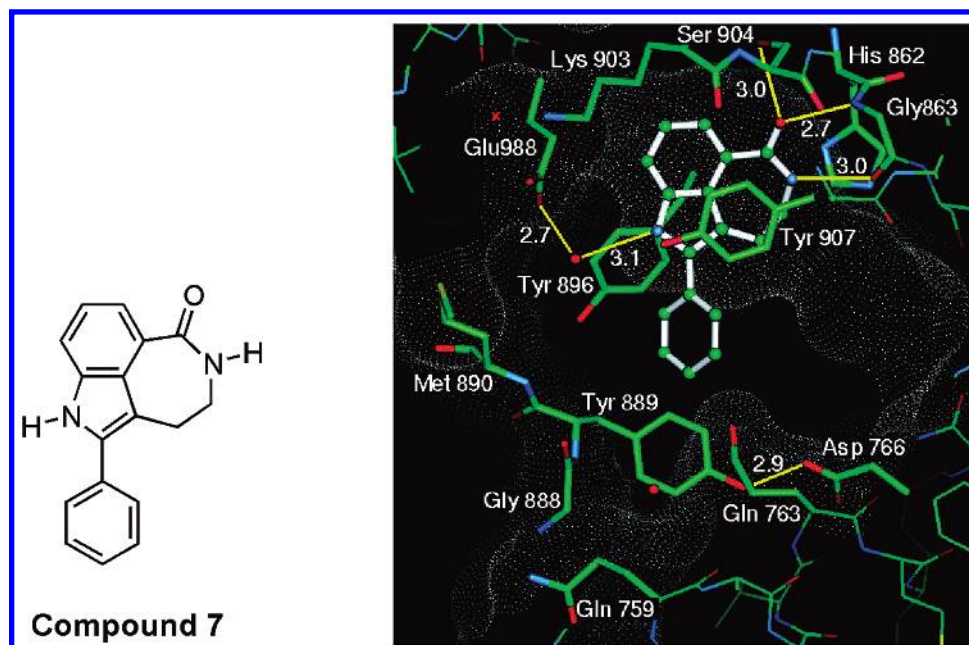


Figure 3. Cocystal structure (2.3 Å resolution) of compound **7** and cPARP-1 CD protein.

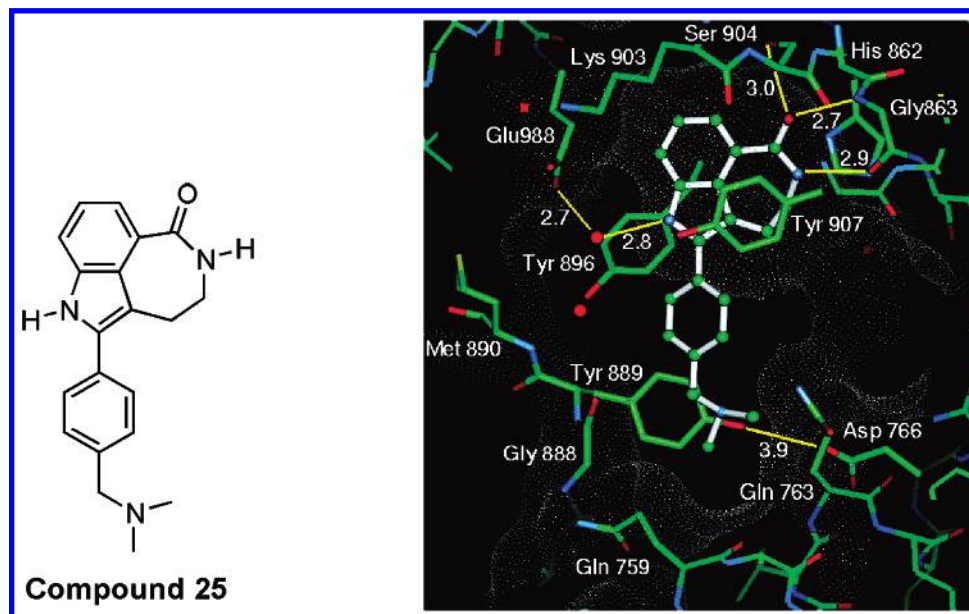


Figure 4. Cocystal structure (2.3 Å resolution) of compound **25** and cPARP-1 CD protein.

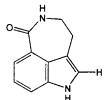
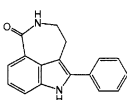
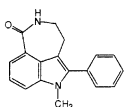
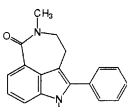
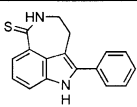
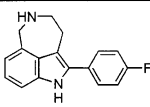
methyl substituent is occupying this space. In fact, the entire loop between Gly-888 and Gly-892 moves away from the ligand to accommodate the alkylamino group. Finally, as seen in Figure 4, an extra water molecule is apparent in the binding site and is situated in the face of the C-2 aryl ring of compound **25**.

Methods

Growth Inhibition Assays. A549 cells (human lung carcinoma, American Type Culture Collection (ATCC), Rockville, MD, or National Cancer Institute, NIH, Bethesda, MD), SW620 cells (human colon carcinoma, ATCC), or LoVo cells (human colorectal cancer, ATCC) were seeded in 96-well plates for 16–24 h before experimental manipulation. To determine the extent of chemosensitization, cells were continuously exposed to increasing concentrations of temozolomide (TM; a gift from the Cancer Research Campaign, Newcastle upon

Tyne, U.K.) or topotecan (TP; SmithKline Beecham Pharmaceuticals, Philadelphia, PA) for 5 days with or without coexposure to 0.4 μ M PARP-1 inhibitor.²⁰ The 0.4 μ M inhibitor concentration displays no intrinsic growth inhibitory activity. At the end of treatments, the relative cell number was determined by the SRB assay.²¹ Data were calculated as a percentage of drug-free (1% DMSO) control or PARP inhibitor alone control. Cell growth IC₅₀ values (concentration of drug required to inhibit cell growth by 50%) were calculated from the generated growth inhibition curves using point-to-point analysis (GraphPad Software, Inc., San Diego, CA). To quantify the potentiation of the cytotoxicity of topotecan (TP) or temozolomide (TM) by test compounds, a dimensionless parameter PF₅₀, the potentiation factor at 50% growth inhibition, was defined as the ratio of IC₅₀ of the control (cytotoxic drug TM or TP alone) to IC₅₀ of the sample (cytotoxic drug plus PARP-1 inhibitor com-

Table 1. PARP-1 Inhibition Observed for [5,6,7]-Tricyclic Indoles^a

Compound No.	Inhibitor	K _i (μM)	Compound No.	Inhibitor	K _i (μM)
3		0.038	7		0.006
29		0.007	30		>10
31		0.057	32		>10

^a K_i values are averages of at least two independent experiments. Experimental variation in K_i values was less than 20% for all compounds.

bination). A PF₅₀ value of 1.0 indicates no effect. Data are normalized to DMSO as a control or to 0.4 μM PARP-1 inhibitor alone as a control.

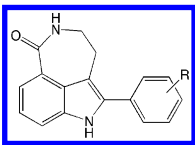
To determine the intrinsic growth inhibitory properties of the compounds in comparison to the minimum concentration required to maximally potentiate TM and TP, cells (LoVo or SW620) grown in 96-well plates were exposed to increasing concentrations of PARP inhibitor in the absence or presence of a concentration of cytotoxic drug that caused <50% inhibition of cell growth, i.e., 400 μM TM, 10 nM TP (LoVo cells), or 2 nM TP (SW620 cells) for 5 days and cell growth was determined by the SRB assay. As appropriate, data were normalized to DMSO control or to TM or TP alone as controls.

NAD⁺ Depletion Assay. A549 cells were treated with MNNG for 20 min in the presence or absence of PARP inhibitors. After the treatment, cells were washed once with 1X Hank's balanced saline solution and extracted with 20% trichloroacetic acid (TCA). The TCA insoluble fraction was removed by centrifugation. The TCA supernatant was extracted with water-saturated ethyl ether to remove TCA. Following removal of TCA, NAD was determined by an enzymatic cycling assay as described,²² and the ADP-ribose polymers were quantified as described.²³

Results and Discussion

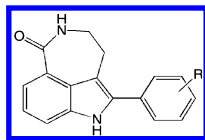
The compounds have been evaluated with an enzymatic activity assay (see Experimental Section, K_i, Tables 1–6) and with in vitro cellular assays that measure the ability of the PARP-1 inhibitors to enhance the effect of cytotoxic agents against cancer cell lines (PF₅₀ values; see Tables 7 and 8). K_i values are averages of at least two independent experiments. Experimental variation in K_i values was less than 20% for all compounds. The 2-phenyl tricyclic indole (**7**, K_i = 6 nM) is approximately 6 times more potent in terms of K_i than the unsubstituted indole (**3**, K_i = 38 nM), suggesting that the C-2 aryl group is interacting favorably at the PARP-1 binding site. The 1-*N*-methylindole (**29**, K_i = 7

Table 2. PARP-1 Activity of Substituted 2-Aryl Tricyclic Indoles

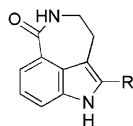
		
compd	R	K _i (μM)
7	H	0.006
8	2-Cl	0.008
9	2-OH	0.023
10	2-SMe	0.032
11	4-OMe	0.006
12	4- ^t Bu	0.029
13	4-F	<0.005
14	4-CF ₃	0.005
15	4-CO ₂ H	0.263
16	3-NH ₂	0.007
17	3-CF ₃	0.006
18	3,5-diCF ₃	0.230

nM) retains potent PARP-1 activity; however, the 1,5-*N,N*-dimethyl analogue (**30**, K_i ≥ 10 μM) is a weak PARP-1 inhibitor. This indicates that the lactam N–H participates in a beneficial interaction with the PARP-1 protein. Additional evidence for the role of the lactam functionality is supported by the relatively weak activity of the thiolactam (**31**, K_i = 57 nM) and the lack of activity for the azatricycle (**32**, K_i ≥ 10 μM). Compound **7** has been cocrystallized with the PARP-1 protein (cPARP-1 CD; see Figure 3). The X-ray structure does show specific interactions of the lactam carbonyl with Ser-904 and Gly-863 and of the lactam –NH with Gly-863. Additionally, the 2-phenyl group may participate in π–π-type interactions with Tyr-907 and Tyr-896 (see Figure 3).

Representative examples of substituted 2-aryl tricyclic indoles and the corresponding PARP-1 enzymatic activity are shown in Table 2. Aryl groups with ortho substituents have reduced PARP-1 activity relative to the other regioisomers, and the activity decreases as the size of the group increases (compounds **8**–**10**), with the 2-thiomethyl (**10**) being a relatively weak PARP-1

Table 3. PARP-1 Activity of Amino-Substituted 2-Aryl Tricyclic Indoles

compd	R	K_i (μ M)
24	3-CH ₂ NMe ₂	0.008
25	4-CH ₂ NMe ₂	0.005
26	4-CH ₂ -(1-pyrrolidinyl)	0.006

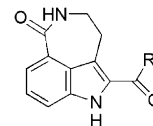
Table 4. PARP-1 Activity of Various 2-Substituted Tricyclic Indoles

compd	R C-2 substituent	K_i (μ M)
35	CN	0.011
39	3-pyridinyl	0.007
40	1-naphthyl	0.005
41	2-biphenyl	0.023
42	2-thiophene	0.005
43	2-pyrrolyl	0.008
44	5-indolyl	0.009

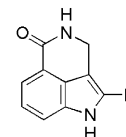
inhibitor ($K_i = 32$ nM). The larger ortho substituent may force the 2-phenyl ring to rotate into an unfavorable conformation that disrupts the binding affinity to PARP-1. Aryl groups substituted at the para position retain PARP-1 activity, similar to the parent (compounds **11**, **13**, and **14**; $K_i \leq 5$ –6 nM). Notable is the slight loss in activity with the para *tert*-butyl substituent (**12**, $K_i = 29$ nM) that indicates a steric restriction at this end of the binding site. The 4-carboxy analogue (**15**, $K_i = 263$ nM) displays comparatively poor PARP-1 activity, possibly due to a repulsive interaction of the negatively charged carboxylate with the protein. Aryl groups with single meta substituents (compounds **16** and **17**; $K_i = 6$ –7 nM) retain good activity; however, the 3,5-bis-CF₃ analogue (**18**) displays poor PARP-1 activity ($K_i = 230$ nM). Analysis of this structure with computational models indicates that there are some unfavorable steric interactions with residues of the protein near the active site. Overall, the PARP-1 binding site appears to be fairly tolerant of a variety of functional groups at each phenyl regioisomer in these new tricyclic inhibitors.

Although the physical properties of the new tricyclic inhibitors were much improved relative to the previously reported bicyclic benzimidazoles, we still sought to enhance the properties by incorporation of an ionizable group on the C-2 aryl substituent. To further enhance the solubility, we explored various amine substituents. Both meta and para aminomethyl substituted 2-aryl tricyclic indole inhibitors retain very favorable PARP-1 activity (Table 3, compounds **24**–**26**; $K_i = 5$ –8 nM). As an example of the improved solubility profile, compound **25** exhibits a water solubility >800 times higher (3.2 mM, pH 7) than the water solubility of the unsubstituted phenyl analogue **7** (0.026 mM, pH 7).

Examination of the X-ray cocrystal structures of the tricyclic inhibitors with PARP-1 indicated that the

Table 5. PARP-1 Activity of 2-Carboxy and Carboxamide Tricyclic Indoles

compd	R	K_i (μ M)
36	NH-Me	0.014
37	NH- <i>i</i> -Pr	0.032
38	NH-Ph	0.010
33	OMe	0.010
34	OH	0.370

Table 6. PARP-1 Activity of [5,6,6]-Tricyclic Indoles

compd	R	K_i (μ M)
2	H	0.047
19	Ph	<0.005
27	(3-CH ₂ NMe ₂)Ph	<0.005
28	(4-CH ₂ NMe ₂)Ph	<0.005

Table 7. Cytotoxicity Potentiation of Topotecan (PF₅₀(TP)) in A549 Cells by PARP-1 Inhibitors

compd	K_i (μ M)	PF ₅₀ (TP) ^a
3	0.038	1.1
7	0.006	1.8
29	0.007	1.7
30	>10	1.2
13	<0.005	2.3
24	0.008	2.1
25	0.005	2.4
26	0.006	2.0
28	<0.005	2.2

^a PF₅₀ is the ratio of IC₅₀ of TP alone to IC₅₀ of TP + PARP-1 inhibitor (0.4 μ M).

protein could accommodate additional functionality at the C-2 position of the indole core. In fact, other C-2 substitution was permissible, including heteroaryls, alkyls, alkynes, carboxamides, and carboxy analogues (Tables 4 and 5). All of the C-2 aryl and heteroaryl substituents shown in Table 4 retain potent-to-moderate PARP-1 activity (**39**–**44**; $K_i = 5$ –23 nM). Similarly, the C-2 cyano-substituted tricycle, **35**, retains PARP-1 activity in the enzymatic assay ($K_i = 11$ nM).

The 2-carboxamide substituted tricyclic indoles exhibit variable PARP-1 activity. Small amides (methyl, **36**; $K_i = 14$ nM) and the aromatic amide (**38**, $K_i = 10$ nM) retain good enzymatic activity; however, a larger alkyl-substituted amide (**37**; $K_i = 32$ nM) shows somewhat reduced PARP-1 activity. The 2-carboxy-substituted tricyclic indoles exhibit even more variable activity. The methyl ester retains potent activity (**33**; $K_i = 10$ nM); however, the carboxylic acid (**34**; $K_i = 370$ nM) is a fairly weak PARP-1 inhibitor.

Representative analogues in the [5,6,6]-tricyclic indole class of PARP-1 inhibitors are shown in Table 6. This class of tricyclic PARP-1 inhibitors displays the same activity trends as those discussed above for the [5,6,7]-tricyclic indole series. The unsubstituted [5,6,6]-tricycle (**2**; $K_i = 47$ nM) exhibits moderate PARP-1 activity, and addition of C-2 aromatic substituents greatly enhances

Table 8. Cellular PARP-1 Activity Influences NAD⁺ and ADP-Polymer Levels^a

monitored cellular activity	DMSO (control)	MNNG alone (25 μ M)	MNNG + 7 (0.4 μ M)	MNNG + 25 (0.4 μ M)	MNNG + 30 ^b (0.4 μ M)
NAD ⁺ levels, %	100	21	81	87	24
% ADP polymer formation	5	100	13	6	105

^a MNNG = 1-methyl-3-nitro-1-nitrosoguanidine, DNA damaging agent; A549 cell line. PARP-1 K_i values (μ M): for **7**, K_i = 0.006; for **25**, K_i = 0.005; for **30**, K_i = 10. ^b Negative control (i.e., very weak PARP-1 inhibitor).

Table 9. Cytotoxicity Potentiation of Topotecan (TP) and Temozolomide (TM) by Compound **26** in Various Cell Lines

cell line	cytotoxic agent ^a	IC ₅₀ cytotoxic agent alone (TP or TM)	IC ₅₀ of TP or TM and 26	PF ₅₀ ^b
A549	TP	24 \pm 1.0 nM	12 \pm 0.5 nM	2.0 \pm 0.1
SW620	TP	3.2 \pm 0.4 nM	1.8 \pm 0.2 nM	1.8 \pm 0.06
LoVo	TP	11.6 \pm 2.0 nM	6.5 \pm 0.4 nM	1.8 \pm 0.2
LoVo	TM	595 \pm 75 μ M	76 \pm 2.3 μ M	7.8 \pm 1

^a TP = topotecan; TM = temozolomide. ^b PF₅₀ = (IC₅₀ of cytotoxic agent alone)/(IC₅₀ of cotherapy (cytotoxic agent plus 0.4 μ M **26**)). Data are mean \pm SEM of three independent experiments.

PARP-1 potency. The C-2 phenyl [5,6,6]-tricycle (**19**; K_i \leq 5 nM) and the two amino-substituted analogues (**27** and **28**; K_i \leq 5 nM) are fairly potent PARP-1 inhibitors.

The ability of these new tricyclic PARP-1 inhibitors to enhance the effects of chemotherapy agents (topotecan (TP) or temozolomide (TM)) is demonstrated here with in vitro cellular growth inhibition assays and the calculation of a potentiation factor (PF₅₀) in various cell lines. A standard concentration of 400 nM PARP-1 inhibitor, which is not intrinsically growth inhibitory, was used. A value of PF₅₀ greater than 1.0 indicates that the PARP-1 inhibitor is capable of enhancing the effects (i.e., further inhibiting cancer cell growth) of the cytotoxic agents (topotecan or temozolomide, Tables 7 and 8). A PF₅₀ value of 1.0 indicates no effect. For this new class of PARP-1 inhibitors, the potentiation factor (PF₅₀) correlates with the K_i data (Table 7). Generally, the PARP-1 inhibitors with a K_i less than 10 nM exhibited good potentiation of TP (PF₅₀ > 1.7). Compounds **7** and **29** potentiate or enhance the effect of topotecan in A549 cells by 1.8 and 1.7 times, respectively. This experiment indicates that the IC₅₀ value of topotecan/PARP-1 inhibitor combination therapy is enhanced relative to topotecan alone in this cell line. (Compound **7** alone is relatively nontoxic with an IC₅₀ of 12 μ M.) The 4-F analogue (**13**) has a favorable potentiation factor (PF₅₀ = 2.3), and this may reflect some increase permeability in the cellular assay. As a class, the amino-substituted tricyclic PARP-1 inhibitors (compounds **24–26**, **28**, Table 7) also displayed favorable potentiation factors with topotecan in A549 cells (PF₅₀ = 2.0–2.4). The weaker PARP-1 inhibitors (**3** and **30**) display little or no potentiation of the cytotoxic agent (PF₅₀ = 1.1–1.2).

A functional assay of PARP-1 activity in A549 cells (which monitors PARP-1-mediated NAD⁺ depletion in cells exposed to DNA alkylating agents) clearly demonstrates that the new compounds inhibit PARP-1 activity in intact cells (Table 8). Cells that are damaged by MNNG and simultaneously treated with the PARP-1 inhibitors, **7** or **25**, are protected from NAD⁺ depletion following the damage. The absence of ADP-polymer formation in these cells after DNA damage and cotreatment with the PARP-1 inhibitor confirms the functional inhibition of PARP-1 by compounds **7** and **25**. Conversely, the weak PARP-1 inhibitor **30** does not prevent

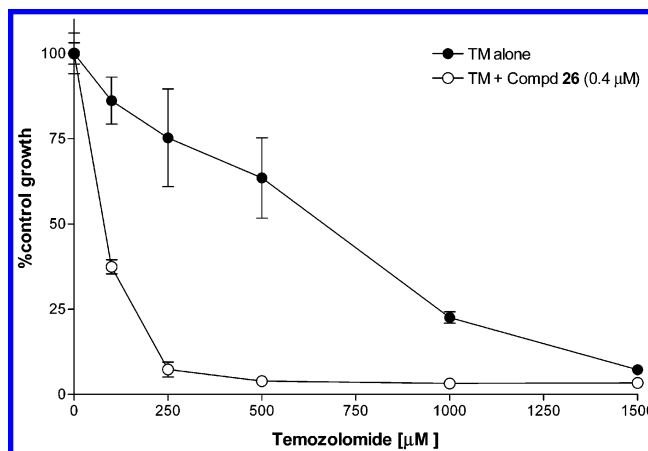


Figure 5. Potentiation of temozolomide (TM) cytotoxicity (growth inhibition) by compound **26** in LoVo cells. Data, normalized to 1% DMSO or 0.4 μ M **26** alone as control, are from a single representative (three total) experiment.

the depletion of NAD⁺ or the production of ADP polymer after treatment with MNNG, similar to the response observed with no PARP-1 inhibitor treatment.

Additional in vitro potentiation experiments were conducted with compound **26**, and the results in various cell lines are summarized in Table 9. This PARP-1 inhibitor, **26**, is capable of enhancing the effects (reduced cell survival) of both topotecan and temozolomide in three separate cell lines (A549, LoVo, and SW690) by factors ranging from 1.8-fold to 7.8-fold.^{10g} Figure 5 illustrates the profound 7.8-fold enhancement of TM-induced growth inhibition achieved by cotreatment with compound **26** (0.4 μ M) in LoVo cells.

Further in vitro experiments illustrate the growth inhibitory (IC₅₀) effect of PARP-1 inhibitor **26** alone and with a sub-IC₅₀ concentration of temozolomide (TM) or topotecan (TP). LoVo cells were exposed to increasing concentrations of PARP inhibitor **26** in the absence or presence of 400 μ M temozolomide or 10 nM topotecan (Figure 6). High concentrations (>1 μ M) of **26** exhibit some intrinsic growth inhibition, but at concentrations that were not intrinsically growth inhibitory, compound **26** significantly increased the temozolomide- and topotecan-induced growth inhibition. Indeed, near-maximal potentiation was achieved at 0.1 μ M **26**, a concentration at least 10 \times lower than the concentration of **26** alone, causing measurable growth inhibition.

Conclusion

A potent new class of tricyclic lactam indole PARP-1 inhibitors have been designed, and an efficient synthesis has been realized. The binding conformation has been evaluated with X-ray cocrystal structures of the ligands and the PARP-1 protein. This new class of PARP-1 inhibitors, represented by compounds **7**, **25** and **26**, displays potent in vitro PARP-1 enzymatic inhibition and potent enhancement of cellular growth inhibition.

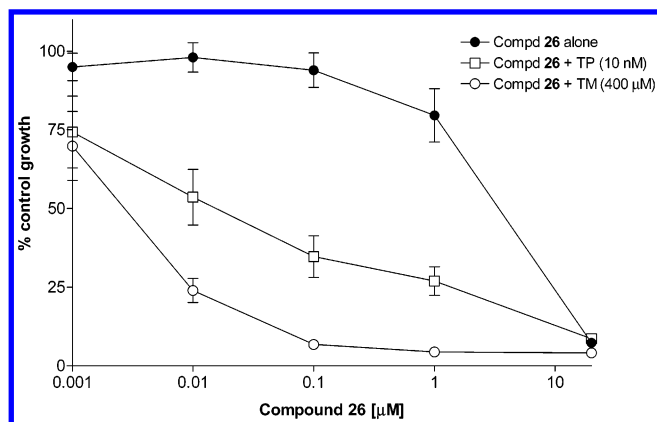


Figure 6. Growth inhibition by compound **26** and TM or TP in LoVo cells. Data are normalized to 1% DMSO, 400 μ M TM, or 10 nM TP alone as control, as appropriate.

Compound **26** with TP displays 1.8- to 2.0-fold enhancement of cellular growth inhibition in several cell lines and a 7.8-fold enhancement of TM-mediated cellular growth inhibition in LoVo cells. The tricyclic analogues also exhibit potent PARP-1 inhibition in a functional assay and are able to inhibit the formation of ADP polymer and to prevent depletion of NAD^+ after cellular insult with a chemotherapy agent. The use of this new class of compounds for potentiation of radiation and chemotherapy is being investigated in in vivo tumor models.²⁴

Experimental Section

PARP-1 Protein Assay Method. Test compounds were incubated in Tris buffer, pH 8.0, with 10 mM MgCl_2 , 1 mM TCEP as a reducing agent, 20 nM hPARP-1 protein, 10 μ g/mL DNase I activated calf thymus DNA (Sigma), 500 μ M NAD^+ , and [^{32}P]- NAD^+ (0.1–0.3 $\mu\text{Ci}/\text{rxn}$) at 25 $^\circ\text{C}$ for 4 min.^{25,26} The reaction was stopped by adding an equal volume of 40% TCA and incubating the mixture on ice for 30 min. The samples were transferred to a Bio-Dot microfiltration apparatus (BioRad), filtered through Whatman GF/C glass fiber filter paper, washed 3 times with 5% TCA and 1% PPI in water, and dried. [^{32}P]-ADP-ribose incorporation into the acid-insoluble material was quantified using a phosphor imager (Molecular Dynamics). Inhibition constants (K_i) were calculated by nonlinear regression analysis.²⁷ Quantitation of K_i values below 5 nM was not possible because of the sensitivity limitations of the assay. K_i values are averages of at least two independent experiments. Experimental variation in K_i values was less than 20% for all compounds.

Determination of Maximum Linear Solubility. The solubility of PARP inhibitors was determined in 5% DMSO/water spectrophotometrically. Concentrated (20 \times) stocks were prepared in 100% DMSO and diluted with distilled water to a final DMSO concentration of 5%. The solutions were allowed to equilibrate for 30 min at room temperature prior to removal of any precipitated inhibitor by centrifugation. The UV-vis spectrum for each sample was recorded, and the absorbance maximum of a selected peak was plotted as a function of theoretical inhibitor concentration. The linear portion of this curve is used to calculate the extinction coefficient of the PARP inhibitor using Beer's law. The maximum linear solubility is determined graphically as the maximal inhibitor concentration in the linear range of the described plot. Solubility in 100% water was determined by stirring a saturated solution of compound in deionized water for 4 h at room temperature ($\sim 22^\circ\text{C}$). Prior to addition of compound, the water was adjusted to pH 7.5 by the addition of Tris buffer, pH 7.5, to a final concentration of 1 mM. The solution was then filtered to remove solid material and analyzed on the spectrophotometer.

Concentration was calculated using the extinction coefficient determined in 5% DMSO/water.

Purification and Crystallization of Chicken PARP-1-CD. The expression, purification, and crystallization of the chicken PARP-1 catalytic domain (cPARP-1-CD) were performed essentially as described with minor modifications.²⁸ Following purification by affinity chromatography using a 3-aminobenzamide affi-gel 10 column, the protein was dialyzed overnight in 50 mM Tris, pH 7.5, 1 mM β -mercaptoethanol, and 1 mM Pefa-bloc (buffer D). The enzyme was further purified by passage over a DEAE-sephacryl column equilibrated in buffer D. The protein does not bind to the column under these conditions, but the remaining major impurity does. The column is washed with two column volumes of buffer D. The flow through and washes were combined, glycerol was added to a final concentration of 20%, and the protein was quick-frozen and stored at -70°C until needed.

Frozen aliquots of cPARP-1-CD were thawed and concentrated 10-fold (to approximately 10 mg/mL) using an Amicon centrprep-10 concentrator. The concentrated protein was diluted with 14 mM β -mercaptoethanol back to the original volume and concentrated again 10-fold. This process was performed twice to remove the glycerol and Pefa-bloc. cPARP-1-CD (6 mg/mL) was combined with 200 μ M PARP-1 inhibitor, centrifuged, and added in a 1:1 ratio with the reservoir solution containing 100 mM Tris, pH 8.5, 8% 2-propanol, and 16–30% PEG 600. Crystallization trials were performed at ambient temperature using the hanging drop vapor diffusion method.

General Experimental Procedure. All solvents were reagent grade or better and used as supplied, unless otherwise indicated. As required, starting materials are azeotropically dried prior to use and reactions were conducted with standard precautions taken to exclude moisture and oxygen. Flash chromatography was accomplished using silica gel (Kieselgel 60, 230–400 mesh). Radial chromatography was performed on a Harrison Research chromatotron with 1, 2, or 4 mm silica gel coated rotors. Thin-layer chromatography utilized Analtech 250 μ m plates with F-256. NMR spectra were recorded in $\text{DMSO}-d_6$, unless otherwise noted, on a GE 300 or a Bruker Advance 300DPX spectrometer. IR spectra were recorded on a Perkin-Elmer 1600 FTIR spectrometer. MS were performed by the Scripps Research Institute MS Facility, at UC Riverside MS Facility, or on an HP 1100 LC/MSD system. Elemental analyses were determined by Atlantic Microlab Inc., Norcross, GA, or Galbraith Laboratories, Nashville, TN. Melting points were taken on a Laboratory Devices melting point apparatus and are reported uncorrected. The tricyclic indole intermediates 3,4,5,6-tetrahydro-1*H*-azepino[5,4,3-*cd*]indol-6-one (**3**) and 3,4-dihydropyrrolo[4,3,2-*de*]isoquinolin-5-(1*H*)-one (**2**) were prepared from methyl indole-4-carboxylate by modification of existing procedures.^{15–17}

Temozolomide (TM) (a gift from the Cancer Research Campaign, Newcastle upon Tyne, U.K.) and topotecan (TP) (SmithKline Beecham Pharmaceuticals, Philadelphia, PA) were dissolved in DMSO at 10 and 2.2 mM, respectively, and stored as aliquots at -20°C . PARP-1 inhibitors were prepared in DMSO at 100 mM and stored at -20°C . Drugs (alone or in combination) were added to cell cultures so that final DMSO concentrations were consistently 1% (v/v).

2-Bromo-3,4-dihydropyrrolo[4,3,2-*de*]isoquinolin-5-(1*H*)-one (Compound 4). Pyridinium tribromide (90%, 0.267 g, 0.75 mmol) was added to a suspension of the [5,6,6]-tricycle **2** (0.086 g, 0.5 mmol) in 40 mL of CH_2Cl_2 at 0°C . The reaction mixture was stirred at 0°C for 30 min. The solvent was removed in vacuo, and ice/water was added to the residue. The resulting suspension was stirred vigorously at 0°C for 30 min and then filtered to give 0.068 g (54%) of a brown solid that was used without further purification. IR (KBr) 3172, 1655, 1606, 1441, 1367, 1292, 755 cm^{-1} ; ^1H NMR (300 MHz, $\text{DMSO}-d_6$) δ 4.61 (s, 2H), 7.17 (app t, $J = 6$ Hz, 1H), 7.32 (d, $J = 6$ Hz, 1H), 7.39 (d, $J = 6$ Hz, 1H), 7.71 (s, 1H), 11.92 (s, 1H); LRMS ($M + H$) 251/253.

2-Bromo-3,4,5,6-tetrahydro-1*H*-azepino[5,4,3-*cd*]indol-6-one (Compound 5). 3,4,5,6-Tetrahydro-1*H*-azepino[5,4,3-

cd]indol-6-one (**3**, 264 mg, 1.42 mmol) in CH_2Cl_2 (30 mL) and THF (30 mL) was treated with pyridinium tribromide (534 mg, 1.67 mmol) at 0 °C. The orange solution was stirred for 10 min and then was allowed to warm to ambient temperature and stirred for an additional hour. Water (30 mL) was added, and the organic solvents were removed in vacuo. The aqueous solution was adjusted to pH 8–9 with 1 M NaOH and extracted with CH_2Cl_2 (3×30 mL). The organic solution was washed with water and brine, dried (Na_2SO_4), filtered, and concentrated. The crude product was recrystallized ($\text{CH}_2\text{Cl}_2/\text{MeOH}$) to yield the tricyclic bromide **5** as a yellow solid: 305 mg (81%); mp 204–206 °C (dec); ^1H NMR (300 MHz, $\text{DMSO}-d_6$) δ 2.85 (m, 2H), 3.45 (m, 2H), 7.25 (t, $J = 7.8$ Hz, 1H), 7.52 (d, $J = 7.8$ Hz, 1H), 7.72 (d, $J = 7.8$ Hz, 1H), 8.14 (br t, 1H), 12.05 (br s, 1H). ^1H NMR (300 MHz, $\text{CDCl}_3/\text{MeOH}-d_4$) δ 2.81 (m, 2H), 3.45 (m, 2H), 7.08 (t, $J = 7.7$ Hz, 1H), 7.34 (d, $J = 7.7$ Hz, 1H), 7.70 (d, $J = 7.7$ Hz, 1H). HRMS (FAB, MH^+) calcd for $\text{C}_{11}\text{H}_{10}\text{BrN}_2\text{O}$: 264.9976. Found: 264.9984.

2-Iodo-1,3,4,5-tetrahydroazepino[5,4,3-*cd*]indol-6-one (Compound 6). 1,3,4,5-Tetrahydroazepino[5,4,3-*cd*]indol-6-one (**3**, 620 mg, 3.35 mmol) was suspended in 80 mL of THF/ CH_2Cl_2 (1:1) and then cooled in an ice bath. Bis[(trifluoroacetoxy)iodo]benzene (1.73 g, 4.02 mmol) and iodine (850 mg, 3.35 mmol) were added, and the reaction mixture was stirred at 0 °C for 25 min. The ice bath was removed, and the reaction mixture was allowed to stir for another 30 min as it warmed to room temperature. The reaction was quenched by addition of aqueous sodium bisulfite. The layers were separated, and the organic layer was dried over MgSO_4 , filtered, and concentrated in vacuo leaving a yellow solid. The crude solid was purified by flash chromatography (5% $\text{MeOH}/\text{CHCl}_3$) to yield 2-iodo-1,3,4,5-tetrahydroazepino[5,4,3-*cd*]indol-6-one, **6**, 308 mg (30%), as a pale-yellow solid. ^1H NMR (300 MHz, $\text{DMSO}-d_6$) δ 2.79 (m, 2H), 3.40 (m, 2H), 7.14 (app t, $J = 7.8$ Hz, 1H), 7.46 (dd, $J = 7.8, 0.6$ Hz, 1H), 7.64 (dd, $J = 7.5, 0.9$ Hz, 1H), 8.06 (br t, 1H), 11.80 (br s, 1H); MS (FAB, MH^+) 313.

2-Phenyl-3,4,5,6-tetrahydro-1*H*-azepino[5,4,3-*cd*]indol-6-one (Compound 7). The tricyclic bromide (**5**, 200 mg, 0.75 mmol) in toluene (20 mL) and EtOH (10 mL) was treated with solid Na_2CO_3 (199 mg, 1.88 mmol), phenylboronic acid (138 mg, 1.13 mmol), and water (0.50 mL). The solution was degassed, and tetrakis(triphenylphosphine)palladium(0) (43 mg, 5 mol %) was added. The solution was heated at reflux for 5 h and then was cooled to ambient temperature and diluted with water (20 mL). The aqueous layer was adjusted to pH 7–8 with saturated aqueous K_2CO_3 and extracted with EtOAc (20 mL $\times 3$). The organic solution was washed with water and brine, dried (Na_2SO_4), filtered, and concentrated. The crude product was recrystallized ($\text{CH}_2\text{Cl}_2/\text{MeOH}/\text{hexanes}$) to yield the 2-phenyltricycle, **7**, as a pale-yellow solid, 183 mg (93%); mp 249–255 °C (dec); ^1H NMR (300 MHz, $\text{CDCl}_3/\text{MeOH}-d_4$) δ 3.14 (m, 2H), 3.53 (m, 2H), 7.23 (t, $J = 7.7$ Hz, 1H), 7.33 (m, 1H), 7.44 (m, 2H), 7.55 (m, 3H), 7.83 (d, $J = 7.7$ Hz, 1H). HRMS (FAB, MH^+) calcd for $\text{C}_{17}\text{H}_{15}\text{N}_2\text{O}$: 263.1184. Found: 263.1189. Anal. ($\text{C}_{17}\text{H}_{14}\text{N}_2\text{O} \cdot 0.8\text{H}_2\text{O}$) C, H, N.

2-(2-Chlorophenyl)-1,3,4,5-tetrahydroazepino[5,4,3-*cd*]indol-6-one (Compound 8). In a manner similar to that described for compound **7**, the tricyclic bromide (**5**, 210 mg, 0.79 mmol) and 2-chlorophenylboronic acid (136 mg, 0.87 mmol) were coupled to yield 2-(2-chlorophenyl)-1,3,4,5-tetrahydroazepino[5,4,3-*cd*]indol-6-one, **8**, 78 mg (33%), as a shiny white solid: mp 275 °C (dec); ^1H NMR (300 MHz, $\text{DMSO}-d_6$) δ 2.76 (m, 2H), 3.38 (m, 2H), 7.23 (apparent t, $J = 7.8$ Hz, 1H), 7.56 (m, 5H), 7.71 (dd, $J = 7.5, 0.9$ Hz, 1H), 8.07 (br t, 1H), 11.53 (br s, 1H); MS (FAB, MH^+) 297. Anal. ($\text{C}_{17}\text{H}_{13}\text{N}_2\text{O} \cdot 0.15\text{H}_2\text{O}$) C, H, N.

2-(2-Hydroxyphenyl)-1,3,4,5-tetrahydroazepino[5,4,3-*cd*]indol-6-one (Compound 9). In a manner similar to that described by Giroux, Han, and Prasit,²⁹ 2-iodophenol (220 mg, 1.00 mmol), pinacol diborane (279 mg, 1.10 mmol), 1,1'-bis-(diphenylphosphino)ferrocenedichloropalladium (24 mg, 0.03 mmol), and potassium acetate (294 mg, 3.00 mmol) were combined in a Schlenk tube. The vessel was evacuated and then refilled with argon thrice. Degassed DMF (6 mL) was

added, and the mixture was stirred at 80 °C under an argon atmosphere for 2 h. 2-Bromo-1,3,4,5,9a,9b-hexahydroazepino[5,4,3-*cd*]indol-6-one (**5**, 239 mg, 0.90 mmol), a second portion of 1,1'-bis(diphenylphosphino)ferrocenedichloropalladium (24 mg, 0.03 mmol), and sodium carbonate (2.5 mL of a 2.0 M aqueous solution, 5.00 mmol) were then added, and the reaction mixture was stirred under an argon atmosphere at 80 °C for another 17 h. The reaction mixture was then poured into 25 mL of water and then was extracted with 25% isopropyl alcohol/ CHCl_3 (3×20 mL). The combined organic extracts were dried (MgSO_4) and concentrated in vacuo, leaving a brown oil. The crude product was passed through a short silica plug with 25% $\text{MeOH}/\text{CHCl}_3$ and then purified by radial chromatography eluting with 20% $\text{MeOH}/\text{CHCl}_3$. Crystallization from $\text{MeOH}/\text{CHCl}_3/\text{hexanes}$ yielded 2-(2-hydroxyphenyl)-1,3,4,5-tetrahydroazepino[5,4,3-*cd*]indol-6-one, **9**, 40 mg (15%), as a white solid: mp 305 °C (dec); ^1H NMR (300 MHz, $\text{DMSO}-d_6$) δ 2.86 (m, 2H), 3.46 (m, 2H), 6.92 (t, $J = 7.5$ Hz, 1H), 7.00 (d, $J = 7.8$ Hz, 1H), 7.16 (t, $J = 7.8$ Hz, 1H), 7.24 (m, 1H), 7.34 (dd, $J = 7.5, 1.2$ Hz, 1H), 7.55 (d, $J = 7.8$ Hz, 1H), 7.66 (d, $J = 7.5$ Hz, 1H), 8.00 (br t, 1H), 9.84 (br s, 1H), 11.20 (br s, 1H); MS (FAB, MH^+) 279. Anal. ($\text{C}_{17}\text{H}_{14}\text{N}_2\text{O}_2 \cdot 0.44\text{CHCl}_3$) C, H, N.

2-(2-Methylsulfanylphenyl)-1,3,4,5-tetrahydroazepino[5,4,3-*cd*]indol-6-one (Compound 10). In a manner similar to that described for compound **7**, the tricyclic bromide (**5**, 530 mg, 2.00 mmol) and 2-thioanisole boronic acid (370 mg, 2.20 mmol) were coupled to yield 2-(2-methylsulfanylphenyl)-1,3,4,5-tetrahydroazepino[5,4,3-*cd*]indol-6-one, **10**, 264 mg (43%), as an off-white solid: mp 271–272 °C; ^1H NMR (300 MHz, $\text{DMSO}-d_6$) δ 2.39 (s, 3H), 2.73 (m, 2H), 3.37 (m, 2H), 7.23 (m, 2H), 7.37 (m, 2H), 7.49 (m, 2H), 7.70 (d, $J = 7.2$ Hz, 1H), 8.05 (br t, 1H), 11.41 (br s, 1H); MS (FAB, MH^+) 309. Anal. ($\text{C}_{18}\text{H}_{16}\text{N}_2\text{OS}$) C, H, N.

2-(4-Methoxyphenyl)-3,4,5,6-tetrahydro-1*H*-azepino[5,4,3-*cd*]indol-6-one (Compound 11). The tricyclic bromide (**5**, 48 mg, 0.18 mmol) in toluene (5 mL) and EtOH (2.5 mL) was treated with solid Na_2CO_3 (48 mg, 0.45 mmol), LiCl (23 mg, 0.54 mmol), *p*-methoxyphenylboronic acid (41 mg, 0.27 mmol), and water (0.25 mL). The solution was degassed, and tetrakis(triphenylphosphine)palladium(0) (10 mg, 5 mol %) was added. The solution was heated at reflux for 13 h and then was cooled to ambient temperature and diluted with water (10 mL). The aqueous layer was adjusted to pH 7–8 with saturated aqueous K_2CO_3 and extracted with EtOAc (10 mL $\times 3$). The organic solution was washed with water and brine, dried (Na_2SO_4), filtered, and concentrated. The crude product was recrystallized (MeOH/THF) to yield the 2-(*p*-methoxyphenyl)tricycle as a white solid, 47.4 mg (89%); mp 143–148 °C (dec); ^1H NMR (300 MHz, $\text{DMSO}-d_6$) δ 3.08 (m, 2H), 3.38 (m, 2H), 3.87 (s, 3H), 7.14 (d of ABq, $J = 8.6$ Hz, 2H), 7.22 (t, $J = 7.5$ Hz, 1H), 7.57 (d, $J = 7.5$ Hz, 1H), 7.64 (d of ABq, $J = 8.6$ Hz, 2H), 7.70 (d, $J = 7.5$ Hz, 1H), 8.11 (br t, 1H), 11.52 (br s, 1H). HRMS (FAB, MH^+) calcd for $\text{C}_{18}\text{H}_{17}\text{N}_2\text{O}_2$: 293.1290. Found: 293.1301. Anal. ($\text{C}_{18}\text{H}_{16}\text{N}_2\text{O}_2$) C, H, N.

2-(4-*tert*-Butylphenyl)-1,3,4,5-tetrahydroazepino[5,4,3-*cd*]indol-6-one (Compound 12). As described for compound **7**, the tricyclic bromide (**5**, 300 mg, 1.13 mmol) and 4-*tert*-butylphenylboronic acid (302 mg, 1.70 mmol) were coupled to yield 2-(4-*tert*-butylphenyl)-1,3,4,5-tetrahydroazepino[5,4,3-*cd*]indol-6-one, **12**, 150 mg (42%), as a white solid: mp 243–244 °C; ^1H NMR (300 MHz, $\text{DMSO}-d_6$) δ 1.33 (s, 9H), 3.05 (m, 2H), 3.38 (m, 2H), 7.20 (app t, $J = 7.8$ Hz, 1H), 7.57 (m, 5H), 7.67 (dd, $J = 7.2, 0.6$ Hz, 1H), 8.07 (br t, 1H), 11.51 (br s, 1H). HRMS (FAB, MH^+) calcd for $\text{C}_{21}\text{H}_{23}\text{N}_2\text{O}$: 319.1810. Found: 319.1813. Anal. ($\text{C}_{21}\text{H}_{22}\text{N}_2\text{O} \cdot 0.3\text{H}_2\text{O}$) C, H, N.

2-(4-Fluorophenyl)-3,4,5,6-tetrahydro-1*H*-azepino[5,4,3-*cd*]indol-6-one (Compound 13). As described for compound **7**, the tricyclic bromide (**5**, 100 mg, 0.54 mmol) and 4-fluorobenzenboronic acid (79 mg, 0.57 mmol) were coupled to yield 2-(4-fluorophenyl)-3,4,5,6-tetrahydro-1*H*-azepino[5,4,3-*cd*]indol-6-one, **13**, 107 mg (99%), as a pale-yellow solid: ^1H NMR (300 MHz, $\text{DMSO}-d_6$) δ 3.04 (m, 2H), 3.38 (m, 2H), 7.22 (app

t, $J = 7.7$ Hz, 1H), 7.39 (m, 2H), 7.56 (dd, $J = 8.0, 0.9$ Hz, 1H), 7.64 (m, 3H), 8.05 (br t, 1H), 11.57 (br s, 1H). HRMS (FAB, MH^+) calcd for $\text{C}_{17}\text{H}_{14}\text{FN}_2\text{O}$: 281.1090. Found: 281.1093. Anal. ($\text{C}_{17}\text{H}_{13}\text{FN}_2\text{O} \cdot 0.6\text{H}_2\text{O}$) C, H, N.

2-(4-Trifluoromethylphenyl)-1,3,4,5-tetrahydroazepino[5,4,3-*cd*]indol-6-one (Compound 14). As described for compound 7, the tricyclic bromide (**5**, 300 mg, 1.13 mmol) and 4-trifluoromethylphenylboronic acid (322 mg, 1.70 mmol) were coupled to yield 2-(4-trifluoromethylphenyl)-1,3,4,5-tetrahydroazepino[5,4,3-*cd*]indol-6-one, 261 mg (70%), as an off-white solid: mp 208–209 °C; ^1H NMR (300 MHz, $\text{DMSO}-d_6$) δ 3.09 (m, 2H), 3.40 (m, 2H), 7.27 (app t, $J = 7.8$ Hz, 1H), 7.60 (dd, $J = 8.1, 0.9$ Hz, 1H), 7.71 (dd, $J = 7.5, 0.6$ Hz, 1H), 7.88 (m, 4H), 8.13 (br t, 1H), 11.77 (br s, 1H); MS (FAB, MH^+) 331. Anal. ($\text{C}_{18}\text{H}_{13}\text{F}_3\text{N}_2\text{O} \cdot 1.0\text{H}_2\text{O}$) C, H, N.

4-(6-Oxo-3,4,5,6,9a,9b-hexahydro-1H-azepino[5,4,3-*cd*]indol-2-yl)benzoic Acid (Compound 15). In a manner similar to that described for compound 7, the tricyclic bromide (**5**, 530 mg, 2.00 mmol) and 4-carboxyphenylboronic acid (365 mg, 2.20 mmol) were coupled to yield 4-(6-oxo-3,4,5,6,9a,9b-hexahydro-1H-azepino[5,4,3-*cd*]indol-2-yl)benzoic acid, 340 mg (56%), as a pale-yellow solid: mp 345.5–346.5 °C (dec); ^1H NMR (300 MHz, $\text{DMSO}-d_6$) δ 3.10 (m, 2H), 3.40 (m, 2H), 7.25 (t, $J = 7.8$ Hz, 1H), 7.59 (dd, $J = 8.1, 0.9$ Hz, 1H), 7.70 (dd, $J = 7.5, 0.6$ Hz, 1H), 7.78 (m, 2H), 8.10 (m, 3H), 11.73 (br s, 1H), 13.00 (br s, 1H); MS (electrospray, MH^+) 307. Anal. ($\text{C}_{18}\text{H}_{14}\text{N}_2\text{O}_3 \cdot 0.9\text{H}_2\text{O}$) C, H, N.

2-(3-Aminophenyl)-3,4,5,6-tetrahydro-1H-azepino[5,4,3-*cd*]indol-6-one (Compound 16). As described for compound 7, the tricyclic bromide (**5**, 428 mg, 1.61 mmol) and 3-aminobenzenboronic acid monohydrate (300 mg, 1.94 mmol) were coupled to yield 2-(3-aminophenyl)-3,4,5,6-tetrahydro-1H-azepino[5,4,3-*cd*]indol-6-one, 110 mg (25%), as an off-white solid: ^1H NMR (300 MHz, $\text{DMSO}-d_6$) δ 3.03 (m, 2H), 3.39 (m, 2H), 5.24 (s, 2H), 6.59 (br d, 1H), 6.78 (d, $J = 7.7$ Hz, 1H), 6.84 (m, 2H), 7.18 (m, 2H), 7.52 (d, $J = 7.9$ Hz, 1H), 7.66 (d, $J = 7.4$ Hz, 1H), 8.04 (br t, 1H), 11.41 (br s, 1H). HRMS (FAB, MH^+) calcd for $\text{C}_{17}\text{H}_{16}\text{N}_3\text{O}$: 278.1293. Found: 278.1297. Anal. ($\text{C}_{17}\text{H}_{15}\text{N}_3\text{O} \cdot 1.1\text{H}_2\text{O}$) C, H, N.

2-(3-Trifluoromethylphenyl)-1,3,4,5-tetrahydroazepino[5,4,3-*cd*]indol-6-one (Compound 17). As described for compound 7, the tricyclic bromide (**5**, 300 mg, 1.13 mmol) and 3-trifluoromethylphenylboronic acid (322 mg, 1.70 mmol) were coupled to yield 2-(3-trifluoromethylphenyl)-1,3,4,5-tetrahydroazepino[5,4,3-*cd*]indol-6-one, 300 mg (80%), as a pale-yellow solid: mp 212.5–213.5 °C; ^1H NMR (300 MHz, $\text{DMSO}-d_6$) δ 3.08 (m, 2H), 3.40 (m, 2H), 7.27 (app t, $J = 7.8$ Hz, 1H), 7.60 (d, $J = 7.8$ Hz, 1H), 7.71 (d, $J = 7.5$ Hz, 1H), 7.77 (m, 2H), 7.96 (m, 2H), 8.13 (br t, 1H), 11.78 (br s, 1H); MS (FAB, MH^+) 331. Anal. ($\text{C}_{18}\text{H}_{13}\text{F}_3\text{N}_2\text{O} \cdot 0.5\text{H}_2\text{O}$) C, H, N.

2-(3,5-Bistrifluoromethylphenyl)-1,3,4,5-tetrahydroazepino[5,4,3-*cd*]indol-6-one (Compound 18). As described for compound 7, the tricyclic bromide (**5**, 300 mg, 1.13 mmol) and 3,5-bistrifluoromethylphenylboronic acid (202 mg, 1.24 mmol) were coupled to yield 2-(3,5-bistrifluoromethylphenyl)-1,3,4,5-tetrahydroazepino[5,4,3-*cd*]indol-6-one, 70 mg (16%), as a pale-yellow solid: mp 230 °C (dec); ^1H NMR (300 MHz, $\text{DMSO}-d_6$) δ 3.11 (m, 2H), 3.42 (m, 2H), 7.31 (app t, $J = 7.8$ Hz, 1H), 7.64 (d, $J = 8.1$ Hz, 1H), 7.73 (d, $J = 7.5$ Hz, 1H), 8.13 (br s, 1H), 8.16 (br t, 1H), 8.28 (br s, 2H), 11.95 (br s, 1H); MS (FAB, MH^+) 399. Anal. ($\text{C}_{19}\text{H}_{12}\text{F}_6\text{N}_2\text{O} \cdot 0.2$ hexanes) C, H, N.

2-Phenyl-3,4-dihydropyrrolo[4,3,2-*de*]isoquinolin-5-(1H)-one (Compound 19). To a suspension of **4** (0.1065 g, 0.424 mmol) in 20 mL of toluene and 10 mL of EtOH was added phenylboronic acid (0.08 g, 0.636 mmol), Na_2CO_3 (0.113 g, 1.06 mmol) dissolved in a minimum amount of water, LiCl (0.054 g, 1.27 mmol), and tetrakis(triphenylphosphine)palladium(0) (24.5 mg, 21.0 μmol). The reaction mixture was refluxed for 16 h. The solvent was removed in vacuo, and the residue was taken up in EtOAc and washed with saturated aqueous NaHCO_3 , H_2O , and brine. The organic layer was dried over Na_2SO_4 and concentrated to give a yellow solid, which was purified by flash column chromatography eluting with a gradient of 20% of EtOAc in hexanes to give 0.098 g (93%) of

the desired product as a yellow solid: mp 215–218 °C (dec); ^1H NMR (300 MHz, $\text{DMSO}-d_6$) δ 5.04 (s, 2H), 7.17 (t, 1H, $J = 7.5$ Hz), 7.34 (d, 1H, $J = 6.6$ Hz), 7.35 (d, 1H, $J = 7.4$ Hz), 7.50 (m, 4H), 7.66 (d, 1H, $J = 7.7$ Hz), 7.84 (s, 1H), 11.64 (s, 1H); HRMS ($\text{M} + \text{H}$) 249.1023.

3-Formylphenyl-3,4-dihydropyrrolo[4,3,2-*de*]isoquinolin-5-(1H)-one (Compound 20). A procedure similar to that described for compound **21** (vide infra) was used to prepare the target aldehyde in 23% yield: ^1H NMR (300 MHz, $\text{DMSO}-d_6$) 5.10 (s, 2H), 7.20–7.23 (m, 1H), 7.36 (d, 1H, $J = 6.0$ Hz), 7.49 (d, 1H, $J = 6.0$ Hz), 7.75–7.77 (m, 1H), 7.86–7.89 (m, 2H), 7.97 (d, 1H, $J = 6.0$ Hz), 8.18 (s, 1H), 10.09 (s, 1H), 11.85 (s, 1H). The aldehyde was used without further purification.

4-Formylphenyl-3,4-dihydropyrrolo[4,3,2-*de*]isoquinolin-5-(1H)-one (Compound 21). To a suspension of the bromide, **4**, in 30 mL of toluene and 15 mL of EtOH was added 4-formylbenzeneboronic acid (0.457 g, 3.05 mmol), Na_2CO_3 (0.538 g, 5.08 mmol) dissolved in a minimum amount of water, LiCl (0.258 g, 6.09 mmol), and tetrakis(triphenylphosphine)palladium(0) (0.117 g, 0.102 mmol). The reaction mixture was refluxed for 48 h. The solvent was removed in vacuo and the residue was taken up in EtOAc and washed with saturated aqueous NaHCO_3 , H_2O , and brine. The organic layer was dried over MgSO_4 and concentrated to give a yellow solid that was purified by flash column chromatography eluting with a gradient of 60–80% of EtOAc in CHCl_3 to give 0.370 g of a mixture of the acetal and the aldehyde. The acetal was converted to the desired product using 5 mL of MeOH in 3 mL of H_2O and a catalytic amount of concentrated H_2SO_4 to give the aldehyde in 66% yield: IR (KBr) 1694, 1653, 1601, 1261, 821, 746 cm^{-1} ; ^1H NMR (300 MHz, $\text{DMSO}-d_6$) 5.09 (s, 2H), 7.26 (t, $J = 6$ Hz, 1H), 7.36 (d, $J = 6$ Hz, 1H), 7.50 (d, $J = 6$ Hz, 1H), 7.85 (d, $J = 9$ Hz, 2H), 7.91 (s, 1H), 8.02 (d, $J = 9$ Hz, 2H), 10.01 (s, 1H), 11.86 (s, 1H); LRMS ($\text{M} + \text{H}$) 277. The aldehyde was used without further purification.

2-(3-Formylphenyl)-3,4,5,6-tetrahydro-1H-azepino[5,4,3-*cd*]indol-6-one (Compound 22). As described for compound 7, the tricyclic bromide (**5**, 381 mg, 1.44 mmol) and 3-formylbenzeneboronic acid (345 mg, 2.16 mmol) were coupled to yield 2-(3-formylphenyl)-3,4,5,6-tetrahydro-1H-azepino[5,4,3-*cd*]indol-6-one, 346 mg (83%), as a tan solid: ^1H NMR (300 MHz, $\text{DMSO}-d_6$) δ 2.86 (m, 2H), 3.16 (m, 2H), 7.01 (t, $J = 7.8$ Hz, 1H), 7.34 (d, $J = 7.3$ Hz, 1H), 7.50 (m, 2H), 7.73 (m, 2H), 7.85 (br t, 1H), 7.94 (s, 1H), 9.88 (s, 1H), 11.50 (br s, 1H). The aldehyde was used without further purification.

2-(4-Formylphenyl)-3,4,5,6-tetrahydro-1H-azepino[5,4,3-*cd*]indol-6-one (Compound 23). As described for compound 7, the tricyclic bromide (**5**, 168 mg, 0.63 mmol) and 4-formylbenzeneboronic acid (142 mg, 0.95 mmol) were coupled to yield 2-(4-formylphenyl)-3,4,5,6-tetrahydro-1H-azepino[5,4,3-*cd*]indol-6-one, 141 mg (77%), as a yellow solid: mp 238–240 °C (dec); ^1H NMR (300 MHz, $\text{DMSO}-d_6$) δ 3.12 (m, 2H), 3.42 (m, 2H), 7.28 (t, $J = 7.6$ Hz, 1H), 7.59 (d, $J = 7.6$ Hz, 1H), 7.62 (d, $J = 7.6$ Hz, 1H), 7.88 (d of ABq, $J = 7.7$ Hz, 2H), 8.05 (d of ABq, $J = 7.7$ Hz, 2H), 8.11 (br t, 1H), 10.07 (s, 1H), 11.75 (br s, 1H). HRMS (FAB, MH^+) calcd for $\text{C}_{18}\text{H}_{15}\text{N}_2\text{O}_2$: 291.1134. Found: 291.1132. The aldehyde was used without further purification.

2-(3-(*N,N*-Dimethylamino)methylphenyl)-3,4,5,6-tetrahydro-1H-azepino[5,4,3-*cd*]indol-6-one (Compound 24). The meta aldehyde **22** (346 mg, 1.19 mmol) in MeOH (40 mL) was treated with dimethylamine (2 M solution in MeOH, 7.16 mmol). The solution was cooled with an ice/water bath and treated dropwise with a solution of sodium cyanoborohydride (82 mg, 1.31 mmol) and zinc chloride (89 mg, 0.66 mmol) in MeOH (10 mL). The resulting solution was adjusted to pH 6–7 with 2 M methanolic HCl. After the mixture was stirred for 30 min, the reaction was quenched with concentrated HCl (0.2 mL) and the methanol was removed by evaporation. The residue was diluted with water (30 mL). The solution was adjusted to pH 10–11 with KOH(s) and extracted with CH_2Cl_2 (30 mL \times 3). The organic solution was washed with water and brine, dried (Na_2SO_4), filtered, and concentrated. The crude product was crystallized ($\text{CH}_2\text{Cl}_2/\text{MeOH}/\text{hexanes}$) to give 2-(3-

(*N,N*-dimethylamino)methylphenyl)-3,4,5,6-tetrahydro-1*H*-azepino[5,4,3-*cd*]indol-6-one, 332 mg (87%), as shiny yellow crystals: mp 222–225 °C; ¹H NMR (300 MHz, DMSO-*d*₆) δ 2.20 (s, 6H), 3.06 (m, 2H), 3.40 (m, 2H), 3.50 (s, 2H), 7.21 (t, *J* = 7.7 Hz, 1H), 7.41 (br d, *J* = 7.4 Hz, 1H), 7.50 (m, 4H), 7.69 (d, *J* = 7.1 Hz, 1H), 8.05 (br t, 1H), 11.56 (br s, 1H). HRMS (FAB, MH⁺) calcd for C₂₀H₂₂N₃O: 320.1763. Found: 320.1753. Anal. (C₂₀H₂₁N₃O·0.25H₂O) C, H, N.

2-(4-(*N,N*-Dimethylamino)methylphenyl)-3,4,5,6-tetrahydro-1*H*-azepino[5,4,3-*cd*]indol-6-one (Compound 25). The aldehyde **23** (310 mg, 1.07 mmol) in MeOH (40 mL) was treated with dimethylamine (2 M solution in MeOH, 6.41 mmol). The solution was cooled with an ice/water bath and treated dropwise with a solution of sodium cyanoborohydride (74 mg, 1.18 mmol) and zinc chloride (80 mg, 0.59 mmol) in MeOH (10 mL). The resulting solution was adjusted to pH 6–7 with 2 M methanolic HCl. After the mixture was stirred for 30 min, the reaction was quenched with concentrated HCl (0.2 mL) and the methanol was removed by evaporation. The residue was diluted with water (30 mL). The solution was adjusted to pH 10–11 with KOH(s) and extracted with CH₂Cl₂ (30 mL × 3). The organic solution was washed with water and brine, dried (Na₂SO₄), filtered, and concentrated. The crude product was crystallized (CH₂Cl₂/MeOH/hexanes) to give 2-(4-(*N,N*-dimethylamino)methylphenyl)-3,4,5,6-tetrahydro-1*H*-azepino[5,4,3-*cd*]indol-6-one, 245 mg (72%), as an off-white solid: mp 226–229 °C (dec); ¹H NMR (300 MHz, DMSO-*d*₆) δ 2.18 (s, 6H), 3.06 (m, 2H), 3.40 (m, 2H), 3.44 (s, 2H), 7.21 (t, *J* = 7.7 Hz, 1H), 7.43 (d of ABq, *J* = 7.9 Hz, 2H), 7.56 (d, *J* = 7.7 Hz, 1H), 7.61 (d of ABq, *J* = 7.9 Hz, 2H), 7.69 (d, *J* = 7.7 Hz, 1H), 8.05 (br t, 1H), 11.53 (br s, 1H). HRMS (FAB, MH⁺) calcd for C₂₀H₂₂N₃O: 320.1763. Found: 320.1753. Anal. (C₂₀H₂₁N₃O·0.55H₂O) C, H, N.

2-(4-Pyrrolidin-1-ylmethylphenyl)-3,4,5,6-tetrahydro-1*H*-azepino[5,4,3-*cd*]indol-6-one (Compound 26). As described for compound **25**, the para aldehyde **23** (150 mg, 0.52 mmol) in MeOH (10 mL) was treated with pyrrolidine (0.26 mL, 3.10 mmol) and a solution of sodium cyanoborohydride (0.57 mmol) and zinc chloride (0.28 mmol) in MeOH (1.1 mL) to give, after recrystallization (CH₂Cl₂/MeOH/hexanes), 2-(4-pyrrolidin-1-ylmethylphenyl)-3,4,5,6-tetrahydro-1*H*-azepino[5,4,3-*cd*]indol-6-one, 141 mg (79%), as pale-yellow solid: mp 221–225 °C (dec); ¹H NMR (300 MHz, DMSO-*d*₆) δ 1.71 (m, 4H), 2.46 (m, 4H), 3.06 (m, 2H), 3.41 (m, 2H), 3.63 (s, 2H), 7.21 (t, *J* = 7.8 Hz, 1H), 7.45 (d of ABq, *J* = 8.2 Hz, 2H), 7.55 (dd, *J* = 7.9, 0.9 Hz, 1H), 7.59 (d of ABq, *J* = 8.2 Hz, 2H), 7.68 (br d, 1H), 8.07 (br t, 1H), 11.54 (br s, 1H). HRMS (FAB, MH⁺) calcd for C₂₂H₂₄N₃O: 346.1919. Found: 346.1911. Anal. (C₂₃H₂₅N₃O·0.5H₂O) C, H, N.

2-(3-Dimethylaminomethylphenyl)-3,4-dihydropyrrolo-[4,3,2-*del*]isoquinolin-5-(1*H*)-one (Compound 27). A procedure, starting with the meta aldehyde **20**, and similar to that described for compound **28** (vide infra) was used to prepare the desired target in 42% yield: ¹H NMR (300 MHz, DMSO-*d*₆) 2.18 (s, 6H), 3.45 (s, 2H), 5.03 (s, 2H), 7.20–7.30 (m, 2H), 7.35 (d, *J* = 6.0 Hz, 1H), 7.40–7.58 (m, 3H), 7.60 (s, 1H), 7.79 (br s, 1H), 11.68 (br s, 1H); HRMS (M⁺) 306.1626.

2-(4-Dimethylaminomethylphenyl)-3,4-dihydropyrrolo-[4,3,2-*del*]isoquinolin-5-(1*H*)-one (Compound 28). To a solution of 2 M dimethylamine in MeOH (0.81 mL, 1.61 mmol) was added 5 N HCl/MeOH (0.11 mL, 0.536 mmol) followed by a suspension of the aldehyde **21** (0.074 g, 0.268 mmol) in 3 mL of MeOH and NaBH₃CN (0.017 g, 0.268 mmol). The resulting suspension was stirred for 72 h at room temperature. Concentrated HCl was added until the pH was less than 2, and the MeOH was removed in vacuo. The residue was taken up in H₂O and extracted with EtOAc. The aqueous solution was brought to about pH 9 with solid KOH and extracted with EtOAc. The organic layer was dried over MgSO₄ and concentrated to give a yellow solid that was purified by flash silica gel chromatography eluting with a gradient of 3% MeOH in CHCl₃ to 10% MeOH/NH₃ in CHCl₃ to give 0.023 g (28%) of an orange solid: ¹H NMR (300 MHz, DMSO-*d*₆) 2.17 (s, 6H), 3.44 (s, 2H), 5.04 (s, 2H), 7.19 (t, *J* = 6 Hz, 1H), 7.33 (d, *J* =

6 Hz, 1H), 7.42 (d, *J* = 6 Hz, 1H), 7.48 (d, *J* = 9 Hz, 2H), 7.63 (d, *J* = 9 Hz, 2H), 7.81 (s, 1H), 11.62 (s, 1H); LRMS (M + H) 306; Anal. (C₁₉H₁₉N₃O·0.75H₂O) C, H, N.

1-*N*-Methyl-2-phenyl-3,4,5,6-tetrahydro-1*H*-azepino-[5,4,3-*cd*]indol-6-one (Compound 29). A solution of the tricyclic 2-phenylindole (compound **7**, 51.3 mg, 0.20 mmol) in THF (1 mL) and DMPU (0.1 mL) was cooled with an ice/water bath and treated dropwise with a suspension of NaH (0.45 mmol) in THF (0.5 mL). The yellow mixture was allowed to stir at 0 °C for 10 min and was treated dropwise with a 1 M solution of MeI in THF (0.22 mL, 0.22 mmol). The mixture was allowed to warm to ambient temperature and stirred for 30 min. The reaction was quenched at 0 °C with saturated aqueous NH₄Cl and extracted with EtOAc (5 mL × 3). The organic solution was washed with water and brine, dried (Na₂SO₄), filtered, and concentrated. The crude product was purified by radial chromatography (2 mm SiO₂, 1–5% MeOH in CH₂Cl₂) to yield the 1-*N*-methylindole tricycle as a white solid: 44.9 mg (81%); mp 254–256 °C (dec); ¹H NMR (300 MHz, DMSO-*d*₆) δ 2.88 (m, 2H), 3.40 (m, 2H), 3.74 (s, 3H), 7.34 (t, *J* = 7.7 Hz, 1H), 7.56 (m, 5H), 7.73 (d, *J* = 7.7 Hz, 1H), 7.80 (d, *J* = 7.7 Hz, 1H), 8.15 (br t, 1H). Anal. (C₁₈H₁₆N₂O·0.75H₂O) C, H, N.

1,5-*N,N*-Dimethyl-2-phenyl-3,4,5,6-tetrahydro-1*H*-azepino[5,4,3-*cd*]indol-6-one (Compound 30). A solution of 2-phenyl-3,4,5,6-tetrahydro-1*H*-azepino[5,4,3-*cd*]indol-6-one (**7**, 0.91 mg, 0.35 mmol) in DMPU (2 mL) and THF (2 mL) was cooled with an ice/water bath and treated with NaH (60%, 0.032 g, 0.80 mmol). The resulting yellow mixture was allowed to stir at 0 °C for 30 min and then was treated with neat MeI (0.88 mmol, 2.5 equiv). The mixture was allowed to warm to room temperature and was stirred for 2 h. The reaction was quenched with aqueous saturated NH₄Cl and extracted with EtOAc (3 × 10 mL). The organic solution was washed with water and brine, dried (Na₂SO₄), filtered, and concentrated to give the crude product as an oil. The crude product was crystallized (THF/hexanes) to give the 1,5-*N,N*-dimethylindole tricycle, 0.090 mg (89%), as an off-white solid: mp 175–177 °C; ¹H NMR (300 MHz, DMSO-*d*₆) δ 2.91 (m, 2H), 3.19 (s, 3H), 3.65 (m, 2H), 3.75 (s, 3H), 7.34 (t, *J* = 7.8 Hz, 2H), 7.58 (m, 5H), 7.72 (d, *J* = 7.8 Hz, 1H), 7.79 (d, *J* = 7.8 Hz, 1H). Anal. (C₁₉H₁₈N₂O·0.5H₂O) C, H, N.

2-Phenyl-1,3,4,5-tetrahydroazepino[5,4,3-*cd*]indole-6-thione (Compound 31). Compound **7** (48.6 mg, 0.18 mmol) in toluene (2 mL) was treated with Lawesson's reagent (75 mg, 0.18 mmol) at room temperature. The solution was heated at reflux for 2 h and then was allowed to cool to room temperature and diluted with water. The mixture was extracted with EtOAc (3 × 5 mL). The organic solution was washed with water and brine, dried (Na₂SO₄), filtered, and concentrated. The crude product was crystallized (CH₂Cl₂/hexanes) to give the thioamide, 34.4 mg (68%), as a yellow solid: mp 223–226 °C (dec); ¹H NMR (300 MHz, DMSO-*d*₆) δ 3.10 (m, 2H), 3.50 (m, 2H), 7.23 (app t, *J* = 7.8 Hz, 1H), 7.57 (m, 1H), 7.61 (m, 3H), 7.69 (m, 2H), 8.19 (d, *J* = 7.6 Hz, 1H), 10.56 (br t, 1H), 11.68 (br s, 1H). HRMS (FAB, MH⁺) calcd for C₁₇H₁₅N₂S: 279.0956. Found: 279.0952. Anal. (C₁₇H₁₄N₂S·0.25H₂O) C, H, N, S.

2-(4-Fluorophenyl)-3,4,5,6-tetrahydro-1*H*-azepino[5,4,3-*cd*]indole (Compound 32). A solution of 2-(4-fluorophenyl)-3,4,5,6-tetrahydro-1*H*-azepino[5,4,3-*cd*]indol-6-one (**13**, 0.206 g, 0.74 mmol) in THF (10 mL) was treated with solid LAH (95%, 0.140 g, 3.68 mmol). The mixture was heated at reflux under argon for 6 h, resulting in a yellow mixture. The mixture was allowed to cool to room temperature and then was cooled further with an ice/water bath. Ice-cold 1 M aqueous HCl (3 mL × 2) was added portionwise and alternating with ice-cold water (3 mL). The mixture was extracted with CH₂Cl₂ (15 mL × 3), washed with water and brine, dried (Na₂SO₄), and concentrated. The crude product was recrystallized (CH₂Cl₂/MeOH/hexanes) to give the azatricycle, 0.142 mg (72%), as a bright, white solid: ¹H NMR (300 MHz, DMSO-*d*₆) δ 3.04 (m, 4H), 4.19 (s, 2H), 6.73 (app d, *J* = 7.2 Hz, 1H), 6.99 (t, *J* = 7.2 Hz, 1H), 7.19 (app d, *J* = 7.2 Hz, 1H), 7.34 (m, 2H), 7.66 (m,

2H), 11.22 (s, 1H). HRMS (FAB, MH^+) calcd for $C_{17}H_{16}FN_2$: 267.1297. Found: 267.1298. Anal. ($C_{17}H_{15}FN_2$) C, H, N.

6-Oxo-3,4,5,6-tetrahydro-1H-azepino[5,4,3-*cd*]indole-2-carboxylic Acid Methyl Ester (Compound 33). 2-Iodo-1,3,4,5-tetrahydroazepino[5,4,3-*cd*]indol-6-one (**6**, 85 mg, 0.28 mmol), palladium tetrakis(triphenylphosphine) (19 mg, 0.02 mmol), and triethylamine (52 mg, 0.51 mmol) were combined in toluene/methanol (8:2 (v/v), 2 mL). Carbon monoxide gas was bubbled through the mixture for 10 min. The reaction mixture was then heated at 85 °C in a sealed tube for 16 h. The solvent was evaporated, and the orange solid was purified by radial chromatography (chloroform to 5% methanol in chloroform). The white solid was recrystallized (chloroform/methanol/hexanes) to yield 6-oxo-3,4,5,6-tetrahydro-1H-azepino[5,4,3-*cd*]indole-2-carboxylic acid methyl ester, 39 mg (100%), as an off-white solid: mp 266–267 °C; 1H NMR (300 MHz, DMSO- d_6) δ 3.25 (m, 2H), 3.43 (m, 2H), 3.89 (s, 3H), 7.38 (app t, J = 7.8 Hz, 1H), 7.61 (dd, J = 8.1, 0.9 Hz, 1H), 7.74 (dd, J = 7.5, 0.9 Hz, 1H), 8.17 (br t, 1H), 11.93 (br s, 1H); MS (FAB, MH^+) 245. Anal. ($C_{13}H_{12}N_2O_3$) C, H, N.

6-Oxo-3,4,5,6-tetrahydro-1H-azepino[5,4,3-*cd*]indole-2-carboxylic Acid (Compound 34). 6-Oxo-3,4,5,6-tetrahydro-1H-azepino[5,4,3-*cd*]indole-2-carboxylic acid octyl ester (prepared in a manner similar to that described for **33** (350 mg, 1.02 mmol)) and lithium hydroxide (122 mg, 5.11 mmol) were dissolved in 10 mL of 2:1 methanol/water and stirred at room temperature for 24 h. The reaction mixture was diluted with water and then washed twice with dichloromethane. The aqueous solution was acidified to ca. pH 2 with concentrated HCl. The white precipitate was collected by filtration, washed with water, and dried in vacuo to yield 6-oxo-3,4,5,6-tetrahydro-1H-azepino[5,4,3-*cd*]indole-2-carboxylic acid, 235 mg (99%), as a white solid: mp 298–299 °C (dec); 1H NMR (300 MHz, DMSO- d_6) δ 3.17 (m, 2H), 3.41 (m, 2H), 7.35 (t, J = 7.8 Hz, 1H), 7.59 (d, J = 8.1 Hz, 1H), 7.73 (d, J = 7.5 Hz, 1H), 8.14 (br t, 1H), 11.77 (br s, 1H), 13.14 (br s, 1H); MS (electrospray, MH^+): 231. Anal. ($C_{12}H_{10}N_2O_3 \cdot 1.0H_2O$) C, H, N.

6-Oxo-3,4,5,6-tetrahydro-1H-azepino[5,4,3-*cd*]indole-2-carbonitrile (Compound 35). In a manner similar to that described by Anderson et al.,³⁰ 2-iodo-1,3,4,5-tetrahydroazepino[5,4,3-*cd*]indol-6-one (**6**, 100 mg, 0.32 mmol), sodium cyanide (31 mg, 0.64 mmol), palladium tetrakis(triphenylphosphine) (19 mg, 0.05 mmol), and copper(I) iodide were combined in a Schlenk tube. The vessel was evacuated and refilled with argon gas three times. Degassed propionitrile (2 mL) was added, and the reaction mixture was stirred at 80 °C under an argon atmosphere for 15 h. The reaction mixture was partitioned between water and 25% $^iPrOH/CHCl_3$. The layers were separated, and the aqueous layer was extracted thrice with 25% $^iPrOH/CHCl_3$. The combined organic layers were dried ($MgSO_4$) and concentrated in vacuo. The yellow solid was recrystallized from $CH_2Cl_2/MeOH/hexanes$ to yield 6-oxo-3,4,5,6-tetrahydro-1H-azepino[5,4,3-*cd*]indole-2-carbonitrile, 38 mg (56%), as a pale-yellow solid: mp 315 °C (dec); 1H NMR (300 MHz, DMSO- d_6) δ 3.04 (m, 2H), 3.47 (m, 2H), 7.46 (t, J = 7.5 Hz, 1H), 7.64 (dd, J = 8.1, 0.9 Hz, 1H), 7.81 (dd, J = 7.2, 0.9 Hz, 1H), 8.24 (br t, 1H), 12.44 (br s, 1H); MS (electrospray, $[M + Na]^+$) 234. Anal. ($C_{12}H_9N_3O$) C, H, N.

6-Oxo-3,4,5,6-tetrahydro-1H-azepino[5,4,3-*cd*]indole-2-carboxylic Acid Methylamide (Compound 36). 6-Oxo-3,4,5,6-tetrahydro-1H-azepino[5,4,3-*cd*]indole-2-carboxylic acid methyl ester (**33**, 50 mg, 0.20 mmol) was suspended in 1 mL of a 33% solution of methylamine in methanol. The suspension was stirred at room temperature for 21 h. Another 2 mL of 33% methylamine in methanol was added, and the resulting solution was stirred for another 8 h at room temperature and then for 15 h at 30 °C. The reaction mixture was concentrated in vacuo, leaving a yellow solid that was crystallized from DMF/ $MeOH/CHCl_3$ to yield 6-oxo-3,4,5,6-tetrahydro-1H-azepino[5,4,3-*cd*]indole-2-carboxylic acid methylamide, 36 mg (72%), as a yellow solid: mp 321–322 °C (dec); 1H NMR (300 MHz, DMSO- d_6) δ 2.81 (s, 3H), 3.15 (m, 2H), 3.40 (m, 2H), 7.32 (app t, J = 7.8 Hz, 1H), 7.61 (d, J = 8.1 Hz, 1H), 7.74 (d, J = 7.5 Hz, 1H), 7.95 (br q, 1H), 8.09 (br t, 1H), 11.46 (br s,

1H); MS (electrospray, $[M + Na]^+$) 266. Anal. ($C_{13}H_{13}N_3O_2 \cdot 0.4H_2O$) C, H, N.

6-Oxo-1,3,4,5-tetrahydro-1H-azepino[5,4,3-*cd*]indole-2-carboxylic Acid Isopropylamide (Compound 37). 6-Oxo-3,4,5,6-tetrahydro-1H-azepino[5,4,3-*cd*]indole-2-carboxylic acid (**34**, 60 mg, 0.26 mmol), isopropylamine (17 mg, 0.29 mmol), and diisopropylethylamine (168 mg, 1.30 mmol) were dissolved in 5 mL of dry DMF. HATU (173 mg, 0.46 mmol) was added, and the resulting mixture was stirred at room temperature under argon for 3 days. The reaction mixture was partitioned between water and 25% $^iPrOH/CHCl_3$. The layers were separated, and the aqueous layer was extracted thrice with 25% $^iPrOH/CHCl_3$. The combined organic layers were dried ($MgSO_4$) and concentrated in vacuo, leaving an off-white solid that was recrystallized from chloroform/methanol to yield 6-oxo-1,3,4,5-tetrahydro-1H-azepino[5,4,3-*cd*]indole-2-carboxylic acid isopropylamide as a white solid: 20 mg (28%); mp 261–262 °C (dec); 1H NMR (300 MHz, DMSO- d_6) δ 1.20 (d, J = 6.6 Hz, 1H), 3.22 (m, 2H), 3.38 (m, 2H), 4.90 (m, 1H), 7.32 (app t, J = 7.8 Hz, 1H), 7.59 (d, J = 8.1 Hz, 1H), 7.71 (d, J = 7.2 Hz, 1H), 7.81 (d, J = 7.5 Hz, 1H), 8.10 (br t, 1H), 11.53 (br s, 1H); MS (electrospray, MH^+) 272. Anal. ($C_{15}H_{17}N_3O_2 \cdot 0.2H_2O$) C, H, N.

6-Oxo-1,3,4,5-tetrahydro-1H-azepino[5,4,3-*cd*]indole-2-carboxylic Acid Phenylamide (Compound 38). In a manner similar to that described for compound **37**, 6-oxo-3,4,5,6-tetrahydro-1H-azepino[5,4,3-*cd*]indole-2-carboxylic acid (**34**, 60 mg, 0.26 mmol) was coupled to aniline (27 mg, 0.29 mmol) to yield 6-oxo-1,3,4,5-tetrahydro-1H-azepino[5,4,3-*cd*]indole-2-carboxylic acid phenylamide as a white solid: 55 mg (69%); mp 320–322 °C (dec); 1H NMR (300 MHz, DMSO- d_6) δ 3.28 (m, 2H), 3.42 (m, 2H), 7.11 (app t, J = 7.5 Hz, 1H), 7.37 (m, 3H), 7.64 (d, J = 8.1 Hz, 1H), 7.74 (m, 3H), 8.15 (br t, 1H), 9.98 (br s, 1H), 11.78 (br s, 1H); MS (electrospray, MH^+) 306. Anal. ($C_{18}H_{15}N_3O_2 \cdot 0.25H_2O$) C, H, N.

2-Pyridin-3-yl-1,3,4,5-tetrahydroazepino[5,4,3-*cd*]indol-6-one (Compound 39). In a manner similar to that described for compound **7**, the tricyclic bromide (**5**, 300 mg, 1.13 mmol) and 3-pyridylboronic acid (153 mg, 1.24 mmol) were coupled to yield 2-pyridin-3-yl-1,3,4,5-tetrahydroazepino[5,4,3-*cd*]indol-6-one, 75 mg (25%), as a light-brown solid: mp 260.5–262.0 °C; 1H NMR (300 MHz, DMSO- d_6) δ 3.07 (m, 2H), 3.40 (m, 2H), 7.25 (app t, J = 7.8 Hz, 1H), 7.57 (m, 2H), 7.71 (dd, J = 7.5, 0.9 Hz, 1H), 8.05 (m, 1H), 8.12 (br t, 1H), 8.59 (m, 1H), 8.88 (m, 1H), 11.75 (br s, 1H); MS (FAB, MH^+) 264. Anal. ($C_{16}H_{13}N_3O \cdot 0.2H_2O$) C, H, N.

2-Naphthalen-1-yl-1,3,4,5-tetrahydroazepino[5,4,3-*cd*]indol-6-one (Compound 40). In a manner similar to that described for compound **7**, the tricyclic bromide (**5**, 300 mg, 1.13 mmol) and 1-naphthaleneboronic acid (214 mg, 1.24 mmol) were coupled to yield 2-naphthalen-1-yl-1,3,4,5-tetrahydroazepino[5,4,3-*cd*]indol-6-one, 70 mg (20%), as an off-white solid: mp 305 °C (dec); 1H NMR (300 MHz, DMSO- d_6) δ 2.70 (m, 2H), 3.38 (m, 2H), 7.25 (app t, J = 7.5 Hz, 1H), 7.61 (m, 5H), 7.75 (dd, J = 7.5, 0.9 Hz, 1H), 7.82 (m, 1H), 8.06 (m, 3H), 11.67 (br s, 1H); MS (FAB, MH^+) 313. Anal. ($C_{21}H_{16}N_2O \cdot 0.2H_2O$) C, H, N.

2-Biphenyl-3-yl-1,3,4,5-tetrahydroazepino[5,4,3-*cd*]indol-6-one (Compound 41). As described for compound **7**, the tricyclic bromide (**5**, 300 mg, 1.13 mmol) and biphenyl-3-boronic acid (213 mg, 0.83 mmol) were coupled to yield 2-biphenyl-3-yl-1,3,4,5-tetrahydroazepino[5,4,3-*cd*]indol-6-one, 116 mg (30%), as an off-white crystalline solid: mp 160–163 °C; 1H NMR (300 MHz, DMSO- d_6) δ 3.13 (m, 2H), 3.42 (m, 2H), 7.24 (app t, J = 7.8 Hz, 1H), 7.42 (m, 1H), 7.61 (m, 7H), 7.79 (m, 2H), 7.94 (b s, 1H), 8.10 (br t, 1H), 11.67 (br s, 1H); MS (FAB, MH^+) 339. Anal. ($C_{23}H_{18}N_2O$) C, H, N.

2-Thiophen-2-yl-1,3,4,5-tetrahydroazepino[5,4,3-*cd*]indol-6-one (Compound 42). In a manner similar to that described for compound **7**, the tricyclic bromide (**5**, 300 mg, 1.13 mmol) and thiophene-2-boronic acid (159 mg, 1.24 mmol) were coupled to yield 2-thiophen-2-yl-1,3,4,5-tetrahydroazepino[5,4,3-*cd*]indol-6-one, 171 mg (56%), as a beige solid: mp 220.5–222.5 °C; 1H NMR (300 MHz, DMSO- d_6) δ 3.08 (m, 2H),

3.48 (m, 2H), 7.23 (m, 2H), 7.52 (m, 2H), 7.69 (m, 2H), 8.05 (br t, 1H), 11.60 (br s, 1H); MS (electrospray, MH^+) 269. Anal. ($\text{C}_{15}\text{H}_{12}\text{N}_2\text{O}_5 \cdot 0.8\text{H}_2\text{O}$) C, H, N.

2-(1H-Pyrrol-2-yl)-1,3,4,5-tetrahydroazepino[5,4,3-cd]-indol-6-one (Compound 43). In a manner similar to that described for compound 7, the tricyclic bromide (**5**, 300 mg, 1.13 mmol) and 1-(*t*-butoxycarbonyl)pyrrole-2-boronic acid (263 mg, 1.24 mmol) were coupled with concomitant removal of the BOC group to yield 2-(1H-pyrrol-2-yl)-1,3,4,5-tetrahydroazepino[5,4,3-cd]indol-6-one, 81 mg (28%), as a greenish gray solid: mp >400 °C (dec); ^1H NMR (300 MHz, $\text{DMSO}-d_6$) δ 3.02 (m, 2H), 3.42 (m, 2H), 6.22 (m, 1H), 6.44 (m, 1H), 6.97 (m, 1H), 7.14 (t, $J = 7.5$ Hz, 1H), 7.49 (dd, $J = 8.1, 0.9$ Hz, 1H), 7.64 (dd, $J = 7.5, 0.6$ Hz, 1H), 7.98 (br t, 1H), 11.01 (br s, 1H), 11.13 (br s, 1H); MS (electrospray, MH^+) 252. Anal. ($\text{C}_{15}\text{H}_{13}\text{N}_3\text{O} \cdot 0.4\text{H}_2\text{O}$) C, H, N.

2-(1H-Indol-5-yl)-1,3,4,5-tetrahydroazepino[5,4,3-cd]indol-6-one (Compound 44). In a manner similar to that described for compound 7, the tricyclic bromide (**5**, 530 mg, 2.00 mmol) and indole-5-boronic acid (354 mg, 2.20 mmol) were coupled to yield 2-(1H-indol-5-yl)-1,3,4,5-tetrahydroazepino[5,4,3-cd]indol-6-one, 396 mg (66%) as a beige solid: mp 315–317 °C (dec); ^1H NMR (300 MHz, $\text{DMSO}-d_6$) δ 3.10 (m, 2H), 3.41 (m, 2H), 6.54 (m, 1H), 7.17 (t, $J = 7.8$ Hz, 1H), 7.42 (m, 2H), 7.55 (m, 2H), 7.68 (d, $J = 7.5$ Hz, 1H), 7.83 (br s, 1H), 8.05 (br t, 1H), 11.26 (br s, 1H), 11.48 (br s, 1H); MS (electrospray, MH^+) 302. Anal. ($\text{C}_{19}\text{H}_{15}\text{N}_3\text{O} \cdot 0.25\text{H}_2\text{O}$) C, H, N.

Crystallography. Purified protein and cocrystals of the C-terminal catalytic domain of chicken PARP were obtained using procedures similar to those previously described.¹⁴ In this study, 100 mM Tris, pH 8.5, 16–30% PEG-600, and 8% isopropyl alcohol were used as the precipitant. X-ray diffraction data were collected at –4 °C using monochromatized Cu K α radiation from a rotating anode generator and a MAR345 image plate. Data were processed with DENZO and SCALEPACK.³¹ The crystal space group is $P2_12_12_1$. For compound **7**, the cell constants are 58.98, 64.76, and 96.88 Å. Data were measured from 20 to 2.3 Å in resolution; 74 743 reflections were scaled and merged into 16 519 unique reflections. The overall R_{merge} is 7.3%, the ratio $I/\sigma(I)$ is 19.1, and the data are 96.7% complete. In the high-resolution shell (2.38–2.30 Å), there are 1619 unique reflections, the overall R_{merge} is 27.8%, the ratio $I/\sigma(I)$ is 4.1, and the data are 96.8% complete. For compound **25**, the cell constants are 59.13, 64.46, and 97.47 Å. Data were measured from 20 to 2.3 Å in resolution; 72 655 reflections were scaled and merged into 17 066 unique reflections. The overall R_{merge} is 7.7%, the ratio $I/\sigma(I)$ is 14.3, and the data are 98.8% complete. In the high-resolution shell (2.38–2.30 Å), there are 1679 unique reflections, the overall R_{merge} is 30.0%, the ratio $I/\sigma(I)$ is 3.4, and the data are 98.8% complete.

These structures of PARP with bound inhibitor were solved by difference maps using the data described above and a model from an earlier structure,^{14c} followed by refinement using the computer program CNX2000.³² For compound **7**, the conventional and free R factors after refinement are 18.1% and 24.0% for 13 485 and 1429 reflections, respectively. The non-hydrogen model contains 2764 protein atoms, 20 inhibitor atoms, and 84 solvent atoms. The root-mean-square (rms) deviations between ideal and model bond distances and angles are 0.006 Å and 1.23°. For compound **25**, the conventional and free R factors after refinement are 18.5% and 24.2% for 13 645 and 1468 reflections, respectively. The non-hydrogen model contains 2764 protein atoms, 24 inhibitor atoms, and 86 solvent atoms. The rms deviations between ideal and model bond distances and angles are 0.006 Å and 1.23°.

Acknowledgment. We thank Gilbert de Murcia for the baculovirus constructs used to produce hPARP-1-FL and cPARP-1-CD for assays and crystallography and also for providing us with protein purification protocols. We thank Michelle Yang for assistance with manuscript preparation.

References

- (1) Ame, J. C.; Rolli, V.; Schreiber, V.; Niedergang, C.; Apiou, F.; Decker, P.; Muller, S.; Hoger, T.; Menissier-de Murcia, J.; De Murcia, G. PARP-2, a novel mammalian DNA damage-dependent poly(ADP-ribose) polymerase. *J. Biol. Chem.* **1999**, *274*, 17860–17868.
- (2) Johansson, M. A human poly(ADP-ribose) polymerase gene family (ADPRTL): cDNA cloning of two novel poly(ADP-ribose) polymerase homologues. *Genomics* **1999**, *57*, 442–445.
- (3) (a) Jean, L.; Risler, J. L.; Nagase, T.; Coulouarn, C.; Nomura, N.; Salier, J. P. The nuclear protein PH5P of the inter-alpha-inhibitor superfamily: a missing link between poly(ADP-ribose)-polymerase and the inter-alpha-inhibitor family and a novel actor of DNA repair? *FEBS Lett.* **1999**, *446*, 6–8. (b) Kickhoefer, V. A.; Siva, A. C.; Kedersha, N. L.; Inman, E. M.; Ruland, C.; Streuli, M.; Rome, L. H. The 193-kD vault protein, VPARP, is a novel poly(ADP-ribose) polymerase. *J. Cell Biol.* **1999**, *146*, 917–928.
- (4) Smith, S.; Giriat, I.; Schmitt, A.; De Lange, T. Tankyrase, a poly(ADP-ribose) polymerase at human telomeres. *Science* **1998**, *282*, 1484–1487.
- (5) Smith, S. The world according to PARP. *TIBS* **2001**, *26*, 174–179.
- (6) (a) Ruf, A.; Rolli, V.; De Murcia, G.; Schulz, G. The mechanism of the elongation and branching reaction of poly(ADP-ribose)-polymerase as derived from crystal structures and mutagenesis. *E. J. Mol. Biol.* **1998**, *278*, 57–65. (b) Kameshita, I.; Matsuda, Z.; Taniguchi, T.; Shizuta, Y. Poly (ADP-ribose) synthetase. Separation and identification of three proteolytic fragments as the substrate-binding domain, the DNA-binding domain, and the automodification domain. *J. Biol. Chem.* **1984**, *259*, 4770–4776.
- (7) (a) D'Amours, D.; Desnoyers, S.; D'Silva, I.; Poirier, G. G. Poly(ADP-ribosylation) reactions in the regulation of nuclear functions. *Biochem. J.* **1999**, *342*, 249. (b) De Murcia, G.; Josiane Murcia, M. D. Poly(ADP-ribose) polymerase: a molecular nick-sensor. *TIBS* **1994**, *19*, 172–176.
- (8) (a) Lautier, D.; Lagueux, J.; Thibodeau, J.; Menard, L.; Poirier, G. G. Molecular and biochemical features of poly (ADP-ribose) metabolism. *Mol. Cell. Biochem.* **1993**, *122*, 171–193. (b) Lindahl, T.; Satoh, M. S.; Poirier, G. G.; Klungland, A. Post-translational modification of poly(ADP-ribose) polymerase induced by DNA strand breaks. *TIBS* **1995**, *20*, 405–411.
- (9) (a) Dantzer, F.; Schreiber, V.; Niedergang, C.; Trucco, C.; Flatter, E.; De La Rubia, G.; Oliver, J.; Rolli, V.; Menissier-de Murcia, J.; De Murcia, G. Involvement of poly(ADP-ribose) polymerase in base excision repair. *Biochimie* **1999**, *81*, 69–75. (b) Durkacz, B. W.; Omidiji, O.; Gray, D. A.; Shall, S. (ADP-ribose) $_n$ participates in DNA excision repair. *Nature* **1980**, *283*, 593–596.
- (10) (a) Kun, E.; Kirsten, E.; Milo, G. E.; Kurian, P.; Kumari, H. L. Cell cycle-dependent intervention by benzamide of carcinogen-induced neoplastic transformation and in vitro poly(ADP-ribose)ylation of nuclear proteins in human fibroblasts. *Proc. Natl. Acad. Sci. U.S.A.* **1983**, *80*, 7219–7223. (b) Borek, C.; Morgan, W. F.; Ong, A.; Celeaver, J. E. Inhibition of malignant transformation in vitro by inhibitors of poly(ADP-ribose) synthesis. *Proc. Natl. Acad. Sci. U.S.A.* **1984**, *81*, 243–247. (c) Boulton, S.; Pemberton, L. C.; Porteous, J. K.; Curtin, N. J.; Griffin, R. J.; Golding, B. T.; Durkacz, B. W. Potentiation of temozolomide-induced cytotoxicity: a comparative study of the biological effects of poly(ADP-ribose) polymerase inhibitors. *Br. J. Cancer*, **1995**, *72*, 849–856. (d) Bowman, K. J.; White, A. W.; Golding, B. T.; Griffin, R. J.; Curtin, N. J. Potentiation of anti-cancer agent cytotoxicity by the potent poly(ADP-ribose)polymerase inhibitors NU1025 and NU1064. *Br. J. Cancer* **1998**, *78*, 1269–1277. (e) Delaney, C. A.; Wang, L.-Z.; Kyle, S.; Srinivasan, S.; White, A. W.; Curtin, N. J.; Calvert, A. H.; Durkacz, B. W.; Newell, D. R. Potentiation of temozolomide and topotecan growth inhibition and cytotoxicity by poly(ADP-ribose) polymerase (PARP) inhibitors in a panel of human cancer cell lines. *Proc. Am. Assoc. Cancer Res.* **1980**, *40*, 402. (f) Delaney, C. A.; Wang, L. Z.; Kyle, S.; White, A. W.; Calvert, A. H.; Curtin, N. J.; Durkacz, B. W.; Hostomsky, Z.; Newell, D. R. Potentiation of temozolomide and topotecan growth inhibition and cytotoxicity by novel poly(adenosine diphosphoribose) polymerase inhibitors in a panel of human tumor cell lines. *Clin. Cancer Res.* **2000**, *6*, 2860–2867. (g) Bowman, K. J.; Newell, D. R.; Calvert, A. H.; Curtin, N. J. Differential effects of the poly(ADP-ribose) polymerase (PARP) inhibitor NU1025 on topoisomerase I and II inhibitor cytotoxicity. *Br. J. Cancer* **2001**, *84*, 106–112.
- (11) Purnell, M. R.; Whish, W. J. D. Novel inhibitors of poly(ADP-ribose) synthetase. *Biochem. J.* **1980**, *185*, 775–777.
- (12) (a) Suto, M. J.; Turner, W. R.; Arundel-Suto, C. M.; Werbel, L. M.; Sebolt-Leopold, J. S. Dihydroisouquinolones: the design and synthesis of a new series of potent inhibitors of poly(ADP-ribose) polymerase. *Anti-Cancer Drug Des.* **1991**, *107*–117. (b) Abdel-

- karim, G. E.; Gertz, K.; Harms, C.; Katchanov, J.; Dirnagl, U.; Szabo, C.; Endres, M. Protective effects of PJ34, a novel, potent inhibitor of poly(ADP-ribose)polymerase (PARP) in in vitro and in vivo models of stroke. *Int. J. Mol. Med.* **2001**, *7*, 255–260.
- (13) (a) Ruf, A.; de Murcia, G. M.; de Murcia, G. M.; Schulz, G. E. Structure of the catalytic fragment of poly(ADP-ribose) polymerase from chicken. *Proc. Natl. Acad. Sci. U.S.A.* **1996**, *93*, 7481–7485. (b) Ruf, A.; de Murcia, G. M.; Schulz, G. E. Inhibitor and NAD⁺ Binding to Poly(ADP-ribose) Polymerase As Derived from Crystal Structures and Homology Modeling. *Biochemistry* **1998**, *37*, 3893–3900.
- (14) (a) Griffin, R. J.; Pemberton, L. C.; Rhodes, D.; Bleasdale, C.; Bowman, K.; Calvert, A. H.; Curtin, N. J.; Durkacz, B. E.; Newell, D. R.; Porteus, J. K.; Golding, B. T. Novel potent inhibitors of the DNA repair enzyme poly(ADP-ribose)polymerase (PARP). *Anti-Cancer Drug Des.* **1995**, *10*, 507–514. (b) Griffin, R. J.; Srinivasan, S.; White, A. W.; Bowman, K.; Calvert, A. H.; Curtin, N. J.; Newell, D. R.; Golding, B. T. Resistance modifying agents. 3. Novel benzimidazole and quinazolinone inhibitors of the DNA repair enzyme poly(ADP-ribose)polymerase. *Pharm. Sci.* **1996**, *2*, 43–47. (c) White, A. W.; Almassy, R.; Calvert, A. H.; Curtin, N. J.; Griffin, R. J.; Hostomsky, Z.; Maegley, K.; Newell, D. R.; Srinivasan, S.; Golding, B. T. Resistance-modifying agents. 9. Synthesis and biological properties of benzimidazole inhibitors of the DNA repair enzyme poly(ADP-ribose) polymerase. *J. Med. Chem.* **2000**, *43*, 4084–4097.
- (15) Clark, R. D.; Repke, D. B. The Leimgruber–Batcho indole synthesis. *Heterocycles* **1984**, *22*, 195–221.
- (16) Kozikowski, A. P.; Hitoshi, I.; Chen, Y.-Y. New synthesis and some selected reactions of the potential ergot alkaloid precursor indole-4-carboxaldehyde. *J. Org. Chem.* **1980**, *45*, 3350–3352.
- (17) Demerson, C. A.; Philipp, A. H.; Humber, L. G.; Kraml, M. J.; Charest, M. P.; Tom, H.; Vávra, I. Pyrrolo(4,3,2-*de*)isoquinolines with central nervous system and antihypertensive activities. *J. Med. Chem.* **1974**, *17*, 1140–1145.
- (18) (a) Flaugh, M. E.; Crowell, T. A.; Clemens, J. H.; Sawyer, B. D. Synthesis and evaluation of the antiovarulatory activity of a variety of melatonin analogues. *J. Med. Chem.* **1979**, *22*, 63–69. (b) Clark, R. D.; Weinhardt, K. K.; Berger, J.; Fisher, L. E.; Brown, C. M.; MacKinnon, A. C.; Kilpatrick, A. T.; Spedding, M. 1,9-Alkano-bridged 2,3,4,5-tetrahydro-1*H*-3-benzazepines with affinity for the α_2 -adrenoceptor and the 5-HT_{1A} receptor. *J. Med. Chem.* **1990**, *33*, 633–641.
- (19) (a) Bowman, R. E.; Evans, E. E.; Guyett, J.; Nagy, H.; Weale, J.; Weyell, D. J.; White, A. C. 1,3,4,5-Tetrahydrobenz[*cd*]indoles and related compounds. II. *J. Chem. Soc., Perkin Trans. 1* **1972**, 1926. (b) Somei, M.; Wakida, M.; Ohta, T. The chemistry of indoles. XLIV. Synthetic study directed toward 3,4,5,6-tetrahydro-1*H*-azepino[5,4,3-*cd*]indoles. *Chem. Pharm. Bull.* **1988**, *36*, 1162–1168.
- (20) For reviews, see the following. (a) Takimoto, C. H.; Wright, J.; Arbuck, S. G. Clinical applications of the camptothecins. *Biochim. Biophys. Acta* **1998**, *1400*, 107–119. (b) Newlands, E. S.; Stevens, M. F. G.; Wedge, S. R.; Wheelhouse, R. T.; Brock, C. Temozolomide: a review of its discovery, chemical properties, pre-clinical development and clinical trials. *Cancer Treat. Rev.* **1997**, *23*, 35–61.
- (21) Skehan, P.; Storeng, R.; Scudiero, D.; Monks, A.; McMahon, J.; Vistica, D.; Warren, J. T.; Bokesch, H.; Kenney, S.; Boyd, M. R. New colorimetric cytotoxicity assay for anticancer-drug screening. *J. Natl. Cancer Inst.* **1990**, *82*, 1107–1112.
- (22) Jacobson, E. L.; Jacobson, M. K. Tissue NAD as a biochemical measure of niacin status in humans. *Methods Enzymol.* **1997**, *280*, 221–230.
- (23) Aboul-Ela, N.; Jacobson, E. L.; Jacobson, M. K. Labeling methods for the study of poly- and mono(ADP-ribose) metabolism in cultured cells. *Anal. Biochem.* **1988**, *174*, 239–250.
- (24) (a) Canan Koch, S.; Webber, S.; Almassy, R.; Boritzki, T.; Calabrese, C.; Curtin, N.; Delaney, C.; Kumpf, B.; Kyle, S.; Li, J.; Maegley, K.; Newell, D.; Thomas, H.; Thoresen, L.; Wang, L.-Z.; Yu, X.-H.; Zhang, K.; Hostomsky, Z. Evaluation of a Potent New Class of Poly(ADP-ribose) Polymerase Inhibitors. Presented at the Keystone Symposium “Cancer, Cell Cycle and Therapeutics”, Steamboat Springs, CO, January 8–13, 2000. (b) Canan Koch, S. S. Design and synthesis of potent PARP-1 inhibitors. Presented at the 221st National Meeting of the American Chemical Society, San Diego, CA, 2001; Paper ORGN-238. (c) Canan Koch, S. S.; Thoresen, L. H.; Tikhe, J. G.; Maegley, K. A.; Li, J.; Yu, X.-H.; Almassy, R. J.; Zhang, K. E.; Zook, S. E.; Kumpf, R. A.; Zhang, C.; Boritzki, T. J.; Calabrese, C. R.; Curtin, N. J.; Delaney, C. A.; Kyle, S.; Thomas, H. D.; Wang, L.-Z.; Newell, D. R.; Hostomsky, Z.; Webber, S. E. Structure–activity relationship, crystal structure, and biological evaluation of potent poly(ADP-ribose) polymerase-1 inhibitors. Presented at the 220th National Meeting of the American Chemical Society, Washington, DC, 2000; Paper MEDI-007.
- (25) Marsischky, G. T.; Wilson, B. A.; Collier, R. J. Role of Glutamic Acid 988 of Human Poly-ADP-ribose Polymerase in Polymer Formation. *J. Biol. Chem.* **1995**, *270*, 3247–3254.
- (26) Simonin, F.; Poch, O.; Delarue, M.; de Murcia, G. Identification of potential active-site residues in the human poly(ADP-ribose)-polymerase. *J. Biol. Chem.* **1993**, *268*, 8529–8535.
- (27) (a) Sculley, M. J.; Morrison, J. F. The determination of kinetic constants governing the slow, tight-binding inhibition of enzyme-catalysed reactions. *Biochim. Biophys. Acta* **1986**, *874*, 44–53. (b) Segel, I. H. *Enzyme Kinetics: Behavior and Analysis of Rapid Equilibrium and Steady-State Enzyme Systems*; John Wiley & Sons: New York, 1975; pp 100–125.
- (28) Jung, S.; Miranda, E. A.; Menissier-de Murcia, J.; Neidergang, C.; Delarue, M.; Schulz, G. E.; de Murcia, G. M. Crystallization and X-ray crystallographic analysis of recombinant chicken poly(ADP-ribose) polymerase catalytic domain produced in Sf9 insect cells. *J. Mol. Biol.* **1994**, *244*, 114–116.
- (29) Giroux, A.; Han, Y.; Prasit, P. One pot biaryl synthesis via in situ boronate formation. *Tetrahedron Lett.* **1997**, *38*, 3841–3844.
- (30) Anderson, B. A.; Bell, E. C.; Ginah, F. O.; Harn, N. K.; Pagh, L. M.; Wepsiec, J. P. Cooperative Catalytic Effects in Palladium-Mediated Cyanation Reactions of Aryl Halides and Triflates. *J. Org. Chem.* **1958**, *23*, 8224–8228.
- (31) Otwinowski, Z.; Minor, W. Processing of X-ray Diffraction Data Collected in Oscillation Mode. In *Methods in Enzymology, Macromolecular Crystallography, Part A*; Carter, C. W., Jr., Sweet, R. M., Eds.; Academic Press: New York, 1997; Vol. 276, pp 307–326.
- (32) Brunger, A. T.; Adams, P. D.; Clore, G. M.; DeLano, W. L.; Gros, P.; Grosse-Kunstleve, R. W.; Jiang, J. S.; Kuszewski, J.; Nilges, M.; Pannu, N. S.; Read, R. J.; Rice, L. M.; Simonson, T.; Warren, G. L. Crystallography & NMR system: A new software suite for macromolecular structure determination. *Acta Crystallogr., Sect. D: Biol. Crystallogr.* **1998**, *54*, 905–921.

JM020259N